The Early Universe: New Aspects of Cuscuton Theory, Modified Dispersion Relations and Pulsar Constraints on Vacuum Noise

by

Hyung Jin Kim

A thesis
presented to the University of Waterloo
in fulfillment of the
thesis requirement for the degree of
Master of Mathematics
in
Applied Mathematics

Waterloo, Ontario, Canada, 2017

I hereby declare that I am the sole author of this thesis. This is a true copy of the thesis, including any required final revisions, as accepted by my examiners.

I understand that my thesis may be made electronically available to the public.

Abstract

The modern cosmology started blossoming in the early 1900s, with the theoretical framework provided by Einstein's general relativity. Soon after that, with observational discoveries such as expansion of cosmos by Hubble or later the CMB (Cosmic Microwave Background), many hypotheses and postulations were made to reconcile the observational data and the theoretical frameworks, and to answer open questions in the field. ΛCDM model with inflation is a model which fits the observational data very well, and is one of the most widely accepted theories. However, this model still leaves us with many puzzles yet to be resolved. In this thesis, the theoretical frameworks and the mathematical tools to understand the modern cosmology will be introduced, along with a brief review of inflation. From there, we will explore three different approaches to address some of these unanswered questions. Furthermore, we will give an example of how observational data can constraint theories of early universe.

Acknowledgements

I would like to thank Prof. Ghazal Geshnizjani, my supervisor, for guiding me and helping me throughout all the projects and this thesis.

I would also like to thank Prof. Niayesh Afshordi and the members of his group meeting for the helpful discussions and ideas. I would also like to thank Supranta Boruah for the useful conversations. I would also like to thank Prof. Amjad Ashoorioon for the helpful discussions and ideas.

Table of Contents

List of Figures

List of Tables

Chapter 1

Introduction

The universe have always been a mystery to mankind. Early philosophers, such as Aristotle and Ptolemy, developed many theories to describe the universe. With the development of science, and mathematical tools along with it, came more accurate models and theories. For example, Copernicus suggested a heliocentric model of the universe, in contract to the Ptolemaic system of universe. Although, the idea of the Sun being the center of the universe does not agree with the current model of physics, this model was based on very crucial principle of relativity. What Copernicus suggested is that the physics on Earth should be the same as the physics on the Sun. This marked a very important advance in the history of cosmology. The Copernicus' principle of relativity also suggests that if the cosmos seems isotropic on Earth then it should also be isotropic at any other points. Although this is not exactly correct, this led to the cosmological principle which views our Universe as homogeneous and isotropic at large scales. The modern cosmology, as we understand it now, took its shape in early 1900s when Albert Einstein developed the general theory of relativity (GR) in 1915. Few years after this theoretical breakthrough, major observational discoveries, including Edwin Hubble's confirmation of expanding universe, followed and the modern cosmology was set afoot.

Cosmology has come a long way since Einstein's time and many models have been developed, disputed, confirmed or disregarded along the way. One of the most widely accepted models of early universe is inflationary cosmology followed by standard big bang nucleosynthesis. This model suggests that our universe went through a period of early accelerated expansion i.e. Inflation, before the radiation dominated phase, and explains some questions such as 'why is our universe largely homogeneous and isotropic,' or 'why is our universe flat'. However, there are still many questions and problems in early universe, such as the initial conditions, the baryonic asymmetry, singularity problem and the cos-

mological constant problem, left yet to be answered and solved. This thesis focuses on the cosmology of early universe, describing some possible theories and approaches in attempts to answer some of these cosmological questions, and how the current observational data can give us information on the early universe.

In chapter 2, mathematical and physical tools, such as the theory of general relativity, will be explained. I will also describe mathematically, how these tools shaped the modern cosmology. Furthermore, in chapter 2, I will discuss some current problems we have with our present models and theories. In chapter 3 to 5, I will explore some attempts to tackle these questions with tools and ideas such as effective field theory, and modified gravity. Chapters 4 to 5 will be based on the papers the author published on or submitted to journals and will have texts, figures, and tables from those papers. Chapter 3 will have texts from *JCAP 1707 (2017) no.07, 022*, chapter 4 will have texts from *JCAP 1709 (2017) 09, 008*, and chapter 5 will have text from *arXiv:1703.05331 [hep-th]*.

Chapter 2

Background

As mentioned in the introduction, this thesis focuses on the universe at early times, and aims to present approaches and attempts to answer cosmological problems. To understand these hypotheses and models, we must also understand the frameworks and tools which shape the modern cosmology.

In this chapter, I will briefly explain general relativity, which is the most widely accepted theory of gravity, and the theory of cosmological perturbations, which describes how quantum fluctuations generate cosmological perturbations. Furthermore, I will also briefly explain a basic idea of inflationary models, and some of the challenges they face.

2.1 General Relativity and Cosmology

General relativity (General Theory of Relativity or GR) was formulated by Albert Einstein in early 1990s. This theory was based on a very different idea of time and gravity than the Newton's idea. In GR, space and time are not separable, and gravity is described by curvatures of space-time. In Newton's picture, space and time are two different quantities and gravity is a real force acting between two massive objectives in a straight line. In this chapter, I will explain some of the mathematical description and important equations in cosmology.

Manifold

To understand how space-time curves, we must first have correct mathematical methods to describe space-time. In general relativity, space-time is considered as a four dimensional manifold. A manifold is a topological space that satisfies following three properties[18]:

- It has countable basis elements (second countable).
- For any two points p and q, one can construct neighborhoods of p and q, which do not intersect with one another (Hausdorff).
- It is locally homeomorphic to Euclidean space.

Tensor

Tensor calculus is a powerful tool that can make calculations of physical quantities on curved manifold much easier. For example, the Riemann tensor conveys information about the curvature of space-time, and the stress-energy tensor describes the density and flux of energy and momentum in space-time.

To understand tensor, we will start by introducing a coordinate function x^α[1], which maps from the space-time manifold to Euclidean $\mathbb{R}^4$. In a coordinate system, we can write a curve γ on space-time, parametrized by λ as $x^\alpha(\lambda)$. Taking a derivative of x^α along the curve gives $dx^\alpha/d\lambda = u^\alpha$. This quantity is a vector which is tangent everywhere to the curve. This vector evaluated at a point $p \in \gamma$ does not lie on the space-time manifold itself, but in a plane tangent to space-time at point p. Under a coordinate transformation from x^α to $\tilde{x}^\beta$, we get[2]

$$\tilde{u}^\beta = \frac{d\tilde{x}^\beta}{d\lambda} = \frac{\partial \tilde{x}^\beta}{\partial x^\alpha}\frac{dx^\alpha}{d\lambda} = u^\alpha \frac{\partial \tilde{x}^\beta}{\partial x^\alpha}. \tag{2.1}$$

Any quantity V^α that transforms as

$$\tilde{V}^\beta = \frac{\partial \tilde{x}^\beta}{\partial x^\alpha} V^\alpha \tag{2.2}$$

is a vector.

[1]The general convention is that Greek indices range from 0 to 3, denoting time and space, and Latin indices range from 1 to 3, denoting only the spatial part of space-time.

[2]Here, we used the Einstein's summation convention. In this convention, when an undefined index appears twice in a single term, we sum over all the values of the index.

If we consider the derivative of a scalar function $f(x^\alpha)$ along the curve γ

$$\frac{df}{d\lambda} = \frac{\partial f}{\partial x^a}\frac{dx^\alpha}{d\lambda}, \tag{2.3}$$

we introduce another object $\partial f/\partial x^\alpha$ called a dual vector. Similarly to the definition of vector above, any quantity U_α that transform as

$$\tilde{U}_\beta = \frac{\partial x^\alpha}{\partial \tilde{x}^\beta} U_\alpha \tag{2.4}$$

is a dual vector. We notice that the contraction of a dual vector with a vector

$$U_\alpha V^\alpha = \frac{\partial x^\alpha}{\partial \tilde{x}^\beta}\tilde{V}^\beta \frac{\partial \tilde{x}^\beta}{\partial x^\alpha}\tilde{U}_\beta = \tilde{U}_\beta \tilde{V}^\beta \tag{2.5}$$

is invariant under coordinate transformations.

With the introduction of vector and dual vector, we can define what a tensor is. A tensor of rank (k, l) is a multi-linear map which takes k number of covector and l number of vectors to $\mathbb{R}$. A rank (k, l) tensor is written as $T^{i_1\ldots i_k}_{j_1\ldots j_l}$. We can consider a vector as a rank $(1, 0)$ tensor, a dual vector as a rank $(0, 1)$ tensor, and a scalar function as a rank $(0, 0)$ tensor.

We must be careful because in general relativity, there are some quantities with indices just like tensors even though these quantities are not tensors. It can be shown that just as vectors and dual vectors, a tensor must always transform in the following way under coordinate transformation:

$$\frac{\partial \bar{x}^\alpha}{\partial x^\mu}\frac{\partial \bar{x}^\beta}{\partial x^\nu} T^{\mu\nu} = \bar{T}^{\alpha\beta}. \tag{2.6}$$

A basic example of this case is a partial derivative of a vector or any tensors. Intuitively, because two tensors at different points live in different tangent planes the combination of these two tensors is not tensorial. In another words, the difference between a vector field A^α at point P with coordinate x^β and at point Q with coordinate $x^\beta + dx^\beta$ is not tensorial:

$$\begin{aligned} dA^\alpha &\equiv A^\alpha(Q) - A^\alpha(P) \\ &= A^\alpha(x^\beta + dx^\beta) - A^\alpha(x^\beta) \\ &= \frac{\partial A^\alpha}{\partial x^\beta} dx^\beta. \end{aligned} \tag{2.7}$$

We can quickly check rigorously that under a coordinate transformation, $\partial A^\alpha/\partial x^\beta$ does not act like a tensor:

$$\frac{\partial \tilde{A}^\mu}{\partial \tilde{x}^\nu} = \frac{\partial}{\partial \tilde{x}^\nu}\frac{\partial \tilde{x}^\mu}{\partial x^\alpha} A^\alpha = \frac{\partial \tilde{x}^\mu}{\partial x^\alpha}\frac{\partial x^\beta}{\partial \tilde{x}^\nu}\frac{\partial A^\alpha}{\partial x^\beta} + \frac{\partial^2 \tilde{x}^\mu}{\partial x^\alpha \partial x^\beta}\frac{\partial x^\beta}{\partial \tilde{x}^\nu} A^\alpha. \tag{2.8}$$

Because of this, we need a different derivative to properly carry a tensor from a point to another.

Covariant Derivative

If we wish to make a generalization of partial derivatives such that on a flat manifold it reduces down to a partial derivative, we can do so by starting from a partial derivative and adding a correction. Since a partial derivative follows two rules, linearity and Leibniz rule, we demand the correction also be linear. It turns out that by introducing an another object called the connection coefficients $\Gamma^{\lambda}_{\mu\alpha}$, we can create an operator which has all the qualifications that we were looking for. We will denote this derivative as D/dx^{μ} and define it as

$$\frac{DV^{\lambda}}{dx^{\mu}} \equiv \frac{\partial}{\partial x^{\mu}} V^{\lambda} + \Gamma^{\lambda}_{\mu\alpha} V^{\alpha}, \tag{2.9}$$

and call it a covariant derivative.

Through out the paper, a partial derivative $\frac{\partial}{\partial x^{\mu}} V^{\nu}$ will be written as $\partial_{\mu} V^{\nu}$ or with a comma $V^{\nu}{}_{,\mu}$. Similarly a covariant derivative $\frac{D}{dx^{\mu}} V^{\lambda}$ will be written as $D_{\mu} V^{\nu}$ or with a semicolon $V^{\nu}{}_{;\mu}$.

Line Element and Metric

One method of mathematically understanding the curvature of space-time is by computing a distance between two points. In a four dimensional flat space-time (known as the Minkowski space-time), the distance between two points(events) can be calculated as

$$(\Delta s)^2 = -(c\Delta t)^2 + (\Delta x)^2 + (\Delta y)^2 + (\Delta z)^2. \tag{2.10}$$

c is a fixed conversion factor between space and time, and it can be shown that electromagnetic waves also propagate at this speed [23]. Throughout this paper we will set $c = 1$.

The infinitesimal distance between two events is called the line element and for the Minkowski space-time, it can be written as

$$ds^2 = -dt^2 + dx^2 + dy^2 + dz^2. \tag{2.11}$$

In general, the local structure of space-time is described through the properties of its line element. The line element in Einstein notation can be written as

$$ds^2 = g_{\mu\nu} dx^{\mu} dx^{\nu}, \tag{2.12}$$

where $g_{\mu\nu}$ is a rank two tensor called metric. The metric tensor can be thought as the tensor which captures the geometric and causal structure of space-time. In Minkowski space-time, the metric in a matrix representation is simply $g_{\mu\nu} = \text{diag}(-1, 1, 1, 1)$ [3].

In general relativity, the metric tensor has following properties:

- The metric is invertible. This means that there exists a tensor $g^{\mu\nu}$ such that $g^{\mu\nu}g_{\nu\alpha} = \delta^{\mu}_{\alpha}$
- Symmetric $g_{\mu\nu} = g_{\nu\mu}$
- Lowers and raises indices of other tensors $g_{\mu\nu}T^{\alpha\nu} = T^{\alpha}{}_{\mu}$

Curvature and Geodesic

Curvature can also be thought as how tangent vectors are affected after transporting them along curves. A connection, $\Gamma^{\lambda}_{\mu\nu}$, introduced in eq. 2.9, connects tangent spaces, thus contains all the information of curvature. Although there are infinitely many connections, under two conditions of symmetry of the connection and metric compatibility of the covariant derivative

$$\Gamma^{\lambda}_{\mu\nu} = \Gamma^{\lambda}_{\nu\mu} \qquad D_{\alpha}g_{\mu\nu} = 0, \tag{2.13}$$

there is a unique connection in Riemannian manifolds called the Levi-Civita connection. This connection can also be constructed from the metric tensor[23]

$$\Gamma^{\lambda}_{\mu\nu} \equiv \frac{1}{2}g^{\lambda\sigma}(\partial_{\mu}g_{\nu\sigma} + \partial_{\nu}g_{\sigma\mu} - \partial_{\sigma}g_{\mu\nu}). \tag{2.14}$$

Every information about the curvature is given by a tensor called the Riemann tensor defined as

$$R^{\sigma}{}_{\rho\mu\nu} = \partial_{\mu}\Gamma^{\rho}_{\nu\sigma} - \partial_{\nu}\Gamma^{\rho}_{\mu\sigma} + \Gamma^{\rho}_{\mu\lambda}\Gamma^{\lambda}_{\nu\sigma} - \Gamma^{\rho}_{\nu\lambda}\Gamma^{\lambda}_{\mu\sigma}. \tag{2.15}$$

The first and the third indices of the Riemann curvature tensor can be contracted to form the Ricci tensor:

$$R_{\mu\nu} \equiv R^{\alpha}{}_{\mu\alpha\nu}. \tag{2.16}$$

The Ricci Tensor can be contracted again using the metric to form the Ricci scalar

$$g^{\mu\nu}R_{\mu\nu} = R^{\mu}{}_{\mu} = R. \tag{2.17}$$

[3] Sign of the components of the metric depends on the convention used. Either $(-,+,+,+)$ or $(+,-,-,-)$ can be used for the sign of the metric

A geodesic is a generalized concept of a straight line in curved spaces. It is the curve that extremizes the distance between two points on a manifold. A parametrized curve $x^\mu(\lambda)$ is a geodesic if it satisfies the geodesic equation

$$\frac{d^2x^\mu}{d\lambda^2} + \Gamma^\mu_{\sigma\rho}\frac{dx^\sigma}{d\lambda}\frac{dx^\rho}{d\lambda} = \kappa(\lambda)\frac{dx^\mu}{d\lambda}, \tag{2.18}$$

where $\kappa = d\ln[\sqrt{\pm(\frac{ds}{d\lambda})^2}]/d\lambda$. The sign choice of ds is given by whether the curve is spacelike (positive) or timelike (negative).

The Einstein Field Equations

So far, we have described curvature and the necessary tools to probe curved space-time. However, we have not talked about the most crucial part of general relativity: how matter and energy are related to the geometry of space-time. The Einstein field equations provide such relations. Einstein's equations are given by

$$G_{\mu\nu} + \Lambda g_{\mu\nu} = \frac{1}{M_p^2}T_{\mu\nu}. \tag{2.19}$$

$G_{\mu\nu}$ is called the Einstein tensor and is defined as

$$G_{\mu\nu} \equiv R_{\mu\nu} - \frac{1}{2}Rg_{\mu\nu}. \tag{2.20}$$

$T_{\mu\nu}$ is the stress energy tensor. It is a rank two tensor with components corresponding to energy density, momentum density, shear stress, pressure, and momentum flux. This tensor contains the information about the matter fields that source the gravitational field in GR. Finally, Λ is referred to as the cosmological constant. Historically, the cosmological constant has been a subject of many debates in the physics community. Currently this quantity presents one of the biggest puzzles in fundamental physics, known as the cosmological constant problem. This will be further discussed later in this thesis.

In GR, Einstein's equations can also be derived from the Einstein-Hilbert action,

$$S = \frac{1}{2M_p^2}\int \sqrt{-g}(R - \Lambda + \mathcal{L}_{matter})\, d^4x, \tag{2.21}$$

where g is the determinant of the metric, R is the contribution from the gravity, $M_p \equiv \frac{1}{\sqrt{8\pi G}}$ is the reduced plank mass, and $\mathcal{L}_{matter}$ is the Lagrangian density of the matter field. The

stress-energy tensor can be obtained from the Lagrangian:

$$T_{\mu\nu} = \frac{-2}{\sqrt{-g}} \frac{\delta(\mathcal{L}_{matter}\sqrt{-g})}{\delta g^{\mu\nu}}. \tag{2.22}$$

Generally, most components of matter and energy in the universe on cosmological scales can be approximated by perfect fluid, thus giving the stress-energy tensor of the form

$$T^{\mu\nu} = (\rho + p)U^{\mu}U^{\nu} + pg^{\mu\nu}. \tag{2.23}$$

Here, ρ represents the matter density, P represents the pressure, and U^{μ} represents the 4-velocity vector of the fluid.

Expanding Universe

As mentioned earlier, Edwin Hubble discovered that our universe is expanding. Therefore, Minkowski metric is not a good description for our universe on large scales. However, given the isotropy and homogeneity of the universe on cosmological scales, Friedmann-Lemaitre-Robertson-Walker (FLRW) metric is the appropriate approximation. The general form of this metric can be written as

$$ds^2 = -dt^2 + a(t)d\Sigma^2, \tag{2.24}$$

where $a(t)$ is called the scale factor and captures the dynamics (expansion and contraction) of the cosmos. Σ corresponds to the spatial part of the manifold, and can be written as a function of three spatial coordinates. In polar coordinates $d\Sigma^2$ can be written as

$$d\Sigma^2 = \frac{dr^2}{1 - \kappa r^2} + r^2(d\theta^2 + \sin\theta d\phi^2), \tag{2.25}$$

where κ represents the curvature of the space[4].

Friedmann Equations

We can plug in the FLRW metric in Einstein's equation, and obtain two equations, namely the Friedmann equations:

$$H^2(t) \equiv \left(\frac{\dot{a}(t)}{a(t)}\right)^2 = \frac{1}{3M_p^2}\rho + \frac{\Lambda}{3} - \frac{\kappa}{a(t)^2}, \tag{2.26}$$

[4]There are different conventions for κ. It can either be taken to have units of length^{-2} or unitless. We can rescale the scale factor such that κ belongs to the set $\{-1, 0, +1\}$ with value depending on negative, zero, or positive curvature respectively. Regardless of the convention, for a perfectly flat space, κ is zero.

and

$$\frac{\ddot{a}(t)}{a(t)} = -\frac{1}{6M_p^2}(\rho + 3p) + \frac{\Lambda}{3}, \tag{2.27}$$

where the quantity $H(t)$ is known as the Hubble constant. These two equations describe the approximate background evolution of the cosmos from the very early time to the present time. We will now turn our attention to the early universe, and briefly discuss the most accepted paradigm for that era, called inflation.

2.2 Inflation

Inflation was developed in 1980s [34] to answer some physical puzzles and problems. Although the theory has its own unanswered questions, it is still considered to be the most successful model to explain much of the current observational data [34] [41].

In this section, we will begin with the standard Hot Big Bang model, and show it's limitation. From there, we will explain how inflationary models resolve those challenges. Finally, we will wrap up this section by presenting the limitations of inflation itself.

2.2.1 Introduction to Hot Big Bang Model

As mentioned before, Hubble discovered that the Universe is currently expanding. Extrapolating from this argument, we arrive at the conclusion that the current observable universe started from a very small, hot, and dense region of space. The idea that universe started from a very hot phase was consolidated by more observational evidences such as abundance of light elements including deuterium, and the discovery of Cosmic Microwave Background (CMB).

To understand the Hot Big Bang model, and its limitations, we begin with a general FLRW metric in spherical coordinate

$$ds^2 = a^2(\tau)\left[-dt^2 + \frac{dr^2}{1-\kappa r^2} + r^2(d\theta^2 + sin^2(\theta)d\phi^2)\right]. \tag{2.28}$$

Here κ belongs to the set $\{-1, 0, 1\}$ and determines the curvature of the spatial hyperplane as hyperbolic, flat, and elliptic respectively.

In our current universe, we have different types of matter and energy (baryons, radiation, dark matter, etc.) contributing to the stress-energy tensor. As mentioned before,

for most of these components, we can approximate the stress-energy tensor to the leading order as

$$T^{\mu\nu(i)} = \text{diag}[-\rho^{(i)}, P^{(i)}, P^{(i)}, P^{(i)}], \tag{2.29}$$

with $\rho^{(i)}$ and $P^{(i)}$ corresponding to energy density and pressure density for each component. To characterize the contributions from different species, we introduce a dimensionless parameter, Ω_i, defined as

$$\Omega_i \equiv \frac{\rho^{(i)}}{3M_p^2 H^2}, \tag{2.30}$$

where the index i represents different species of matter. The Friedmann equations (eq. 2.26) implies that

$$\sum_i \Omega_i = \Omega_{tot} = 1 + \frac{\kappa}{a^2 H^2}. \tag{2.31}$$

To see how each type of matter contributes to the evolution of universe, we start with the continuity equation, which can be derived from the energy-momentum conservation of each species ($T^{\mu\nu(i)}_{\ \ ;\nu} = 0$),

$$\dot{\rho}^{(i)} + 3H(\rho^{(i)} + P^{(i)}) = 0. \tag{2.32}$$

For all of these components, relativistic or non-relativistic, one can show that the equations of state can be approximated by

$$P^{(i)} \approx w^{(i)} \rho^{(i)}, \tag{2.33}$$

where $w^{(i)}$ is some constant. For example, for non-relativistic particles, $w = 0$ and for relativistic particles such as photons (radiation), $w = 1/3$. Substituting eq. 2.33 into eq. 2.32, we get

$$\rho^{(i)} \propto a^{-3(1+w^{(i)})}. \tag{2.34}$$

For $\kappa = 0$, and when one particular component dominates over other components, we get

$$a(t) \propto \begin{cases} t^{\frac{2}{3(1+w^{(i)})}} & w^{(i)} \neq -1 \\ e^{Ht} & w^{(i)} = -1. \end{cases} \tag{2.35}$$

From the above equations, we can see that for radiation we have, $a^{(\gamma)}(t) \propto t^{1/2}$ and $\rho^{(\gamma)} \propto a^{-4}$, and for non-relativistic matter (dust), we have $a^{(m)}(t) \propto t^{2/3}$ and $\rho^{(m)} \propto a^{-3}$ [41].

Historically, it was evident to cosmologists from very early on that the density of non-relativistic particles was much higher than the relativistic particles in the present universe. However, comparing the energy density evolution of radiation and matter, we can see that as $a(t)$ goes to smaller values, radiation must have dominated over the matter density

in the background evolution. This implies that the universe was dominated by radiation phase preceding the matter dominated phase. This model was referred to as the standard Hot Big Bang model. It suggests that the universe originated from a very hot, dense and a small region, and went through different phases of expansion. With evidence such as the discovery cosmic background radiation (Penzias and Wilson, 1964 [47]), or the number of light elements (helium, deuterium, etc.), this model was in good agreement with the observations.

2.2.2 Shortcomings of Hot Big Bang Model

Even with all its successes, the Hot Big Bang model faced some fundamental challenges. Here, we present couple of these problems.

Flatness Problem

When we look at the equation 2.31, we can consider the term $\Omega_\kappa \equiv \frac{\kappa}{a^2H^2}$ as the contribution from the curvature of the Universe. In late 1900s, cosmologists noticed that the ratio between the curvature contribution and the matter contribution is order of 1:

$$\frac{\Omega_\kappa}{\Omega_m} \leq 1. \tag{2.36}$$

However, since $\Omega_\kappa/\Omega_m \propto a$, one can easily see that as $a \to 0$ in the early times, Ω_κ gets extremely fine tuned. In fact, the actual calculation showed that Ω_κ had to be less than 10^{-60} around the Planck time. So the question arises: why was κ so small in the very early Universe?

Horizon Problem

In the Hot Big Bang model, the universe started from a very dense, small region. In the very early times, the universe was so dense and hot, the matter content was ionized (i.e. free protons and electrons) and the radiation was scattered very efficiently by matter. In other words, the universe was completely opaque to radiation. As universe cooled down, the electrons and protons could combine into atoms. This phase is called the recombination. During this period, the universe cooled down enough so that ions combined into neutral hydrogens and the mean free paths of photons became larger than the size of the observable

universe. The CMB radiation we observe today is the photons traveling to us from this era, called the last scattering surface.

The Horizon Problem arises from the homogeneity of the CMB temperature to precision of 10^{-5} at last scattering surface. To probe this problem, consider a photon radial trajectory within the flat FRLW metric, given by $a(t)dr = dt$. We can integrate both sides to get a

$$r = \int_{t_i}^{t} \frac{dt'}{a(t')} = \int_{a(t_i)}^{a(t)} \frac{da}{a^2 H}, \tag{2.37}$$

where t_i is the initial time. Therefore, the physical size of causal horizon (light cone) at time t is given by

$$d_H(t) = ar = a(t) \int_{a(t_i)}^{a(t)} \frac{da}{a^2 H}. \tag{2.38}$$

Now, looking at the Friedmann equations 2.26, we can show that

$$H(t) = H_0 \sqrt{\sum_i \Omega_{i,0} a^{-3(1+\omega^{(i)})}}, \tag{2.39}$$

where the subscript 0 denote the value of the corresponding parameter in the present day. For the matter dominated universe, we have $H = H_0\sqrt{\Omega_{m,0}a^{-3}}$, and for the radiation dominated universe, we have $H = H_0\sqrt{\Omega_{\gamma,0}a^{-4}}$. As we mentioned before the universe must have been radiation dominated preceding matter phase. The time when the contributions from radiation and matter density were equal can easily be calculated by taking into account the present time density of each which leads to $a_{eq} \sim 1/3000$. Thus we can separate the integral into two part to evaluate the size of horizon at surface of last scattering

$$d_H(t_{LS}) = a(t) \left[\int_{a_i}^{a_{eq}} \frac{da}{a^2 H} + \int_{a_{eq}}^{a_{LS}} \frac{da}{a^2 H} \right] \tag{2.40}$$

where subscripts i, eq, LS correspond to values at initial time, at the equal density time, and at the surface of last scattering. The first term is for the radiation dominated era and the second term is for the matter dominated era. Now writing H in terms of the scale factor a, we can compute the physical distance from the beginning of the universe to the

last scattering:

$$d_H(t) = a(t)\left[\int_{a_i}^{a_{eq}} \frac{da}{a^2(H_0\sqrt{\Omega_{\gamma,0}a^{-4}})} + \int_{a_{eq}}^{a_{LS}} \frac{da}{a^2(H_0\sqrt{\Omega_{m,0}a^{-3}})}\right] \tag{2.41}$$

$$= a(t)\left[\int_{a_i}^{a_{eq}} \frac{da}{(H_0\sqrt{\Omega_{\gamma,0}})} + \int_{a_{eq}}^{a_{LS}} \frac{da}{a^{1/2}(H_0\sqrt{\Omega_{m,0}})}\right] \tag{2.42}$$

$$= a(t)\left[\frac{a_{eq}}{H_0\sqrt{\Omega_{\gamma,0}}} + 2\frac{a_{LS}^{1/2} - a_{eq}^{1/2}}{H_0\sqrt{\Omega_{m,0}}}\right]. \tag{2.43}$$

Here we took $a_i = 0$, which would be mathematically the smallest value[5]. It is often more convenient to write these calculations in terms of redshift, z given by

$$z = \frac{1}{a} - 1. \tag{2.44}$$

By plugging in the current values of $\Omega_{\gamma,0} \sim 10^{-4}$, $\Omega_{m,0} \sim 0.3$, $H_0 \sim 70$km/s/Mpc, $z_{eq} \sim 3000$, and $z_{LS} \sim 1100$, we can compute the value of the causal horizon at the time of last scattering to be about $d_{H,ls} \sim 0.001$ Mpc. Two points separated by $d_{H,ls}$ at $z \sim 1100$ will now be separated by $1100 \times d_{H,ls} \sim 1$ Mpc due to the expansion of the universe. However, we can measure temperature of CMB on cosmological scales $\sim 10^4$ Mpc. In other words the causal horizon at the time of last scattering corresponds only to about 10^{-4} radian angle of the sky. This means that less than 1 angular degree of the sky was in causal contact at the end of recombination era. However, in the CMB data, is homogenous to one in 10^5 on all cosmological scales, which indicates correlations on the scales that had not been in casual contact. This is called the Horizon problem.

Solution: Accelerated Expansion Phase

Some of the above problems can be answered if we consider a scenario where the universe undergoes a phase of accelerated expansion. Here we will briefly explain how the horizon problem can be solved in this model. Later in the thesis, we will also explain how the flatness problem can be solved. To achieve this, consider the size of comoving horizon at time t :

$$r = \int_{r(t_i)}^{r(t)} \frac{dt'}{a(t')} = \int_{a(t_i)}^{a(t)} \frac{da}{a^2 H} = \int_{\ln a_i}^{\ln a} R_H \; d\ln a, \tag{2.45}$$

[5]From physical of point of view we couldn't extend the theory all the way to that limit as energy densities become super Planckian. However, for the following argument as we see the exact value of lower limit of the integral doesn't make much difference.

where we we define the Hubble radius as

$$R_H = 1/(aH). \tag{2.46}$$

As we see from eqs. 2.39 and 2.35, for radiation $R_H \propto a = e^{\ln a}$. This means as $a \to 0$, the contribution from early universe to causal horizon is exponentially suppressed and integral is dominated by upper bound. Note that during radiation and later, matter era, the dependence of R_H to a (or redshift) is determined by density of radiation and matter in the universe (see eqs 2.39, 2.46) which is fixed by Big Bang Nucleosynthesis (BBN). Therefore we can not solve the problem by changing the history of universe after BBN, during the radiation phase or after that. However, if we have a pre-radiation phase during which R_H doesn't decay away as $a \to 0$ or in other words, R_H was bigger at very early times, then we could make the size of comoving horizon much bigger.

That means during that phase R_H decreases with time. In other words, we need a period of time where

$$\frac{d(aH)^{-1}}{dt} < 0 \Rightarrow -\frac{1}{a} - \frac{\dot{H}}{H^2}\frac{1}{a} < 0 \Rightarrow \ddot{a} > 0. \tag{2.47}$$

This leads to the conclusion that Universe must have gone under a phase of acceleration, now known as inflation.

2.2.3 Inflation, the Acceleration Phase

From the second Friedmann equation, eq 2.27, we can see that for the accelerating phase ($\ddot{a} > 0$) to happen, we need an equation of state that satisfies the inequality

$$p < -\frac{1}{3}\rho. \tag{2.48}$$

One of the simplest example of sources achieving this relation is cosmological constant, corresponding to the equation of state

$$p = -\rho. \tag{2.49}$$

From the equation 2.35, we see that under the above condition, the scale factor grows exponentially in time, $a(t) \propto e^{Ht}$, which corresponds to a space-time manifold, called de Sitter space-time. Note that in this space-time, we have the light-like trajectory

$$r = \int \frac{dt}{a} = \int e^{-Ht} dt = -\frac{1}{e^{Ht} H} \Rightarrow a \sim \frac{1}{r\ H} \tag{2.50}$$

However, setting a strict cosmological constant leads to a never-ending acceleration of the universe that does not enter a radiation era. As we will show in the following subsections, we can get approximately that equation of state leading to quasi-de Sitter space-time by introducing a scalar field, called inflaton field.

Inflation

To begin with, consider a scalar field, Π, and its potential, $V(\Pi)$, minimally coupled to gravity. The action is given by

$$S_\Pi = \int dx^4 \sqrt{-g}(-\frac{1}{2}\partial_\mu \Pi \partial^\mu \Pi - V(\Pi)). \tag{2.51}$$

Varying this action with respect to the metric, we get the stress-energy tensor

$$T_{\mu\nu} = \partial_\mu \Pi \partial_\nu \Pi - g_{\mu\nu}\left(\frac{1}{2}\partial^\sigma \Pi \partial_\sigma \Pi + V(\Pi)\right). \tag{2.52}$$

In FLRW universe, where the metric and the scalar field, $\Pi(t)$, are assumed to be homogeneous and isotropic, the energy density is given by

$$\rho = -T^0{}_0 = \frac{1}{2}\dot{\Pi}^2 + V(\Pi), \tag{2.53}$$

and the pressure is given by

$$p = \frac{1}{2}\dot{\Pi}^2 - V(\Pi). \tag{2.54}$$

Furthermore, we can obtain the equation of motion from varying the action (the Euler-Lagrange equation):

$$\ddot{\Pi} + 3H\dot{\Pi} + V'(\Pi) = 0, \tag{2.55}$$

where $V'(\Pi)$ is the derivative with respect to the scalar field Π. Computing the time-time component of Einstein equations leads to the following Friedmann equation:

$$H^2 = \frac{1}{3M_p^2}(\frac{1}{2}\dot{\Pi}^2 + V(\Pi)) - \frac{\kappa}{a^2} \tag{2.56}$$

From these two equations we also can derive another useful equation

$$\dot{H} = -\frac{1}{2M_p^2}\dot{\Pi}^2 + \frac{\kappa}{a^2}. \tag{2.57}$$

Here, κ, the curvature of space-time, can be neglected because it is not the dominant term, and it becomes extremely small. These are the systems of equations governing the dynamics of homogeneous and isotropic scalar field in flat FRLW space-time and the corresponding cosmological geometry [41].

The Slow-Roll Regime

The system of equations (2.56 - 2.57) does not always ensure an accelerated expansion of the universe[41]. To obtain such acceleration, we work in a regime called the slow-roll approximation.

As mentioned, we want the equation of state to look like $p \approx -\rho$. From the eqs. 2.54 and 2.53, we can achieve that equation of state, if the potential is much greater than the kinetic term:

$$|V(\Pi)| \gg \frac{1}{2}\dot{\Pi}^2. \tag{2.58}$$

Then from the Friedmann equations, we see that

$$H^2 \approx \frac{1}{3M_p^2}V(\Pi) \tag{2.59}$$

and

$$\dot{H} = -\frac{1}{2M_p^2}\dot{\Pi}^2. \tag{2.60}$$

From these two equations, and the requirement that the potential must be much bigger than the kinetic term, comes the first slow roll parameter ϵ and its condition:

$$\epsilon \equiv -\frac{\dot{H}}{H^2} \ll 1. \tag{2.61}$$

Now, we need another condition that will allow inflation to happen for a long enough period. This means that we need the change in the kinetic energy to be much less than the change in the potential energy:

$$\frac{d}{dt}\left(\frac{1}{2}\dot{\Pi}^2\right) \ll (V(\dot{\Pi})) \Rightarrow \dot{\Pi}\ddot{\Pi} \ll \partial_\Pi V\dot{\Pi}. \Rightarrow \ddot{\Pi} \ll V'(\Pi). \tag{2.62}$$

Imposing the first slow-roll approximation, $\dot{\Pi}^2 \ll V$, the Friedmann equations give us the relations

$$V'(\Pi) \approx \frac{2M_p^2 H\dot{H}}{\dot{\Pi}} \tag{2.63}$$

and

$$\ddot{H} = -\frac{1}{M_p^2}\dot{\Pi}\ddot{\Pi} \Rightarrow \ddot{\Pi} = \frac{-M_p^2\ddot{H}}{\dot{\Pi}}. \tag{2.64}$$

The above equations gives us the second slow-roll parameter η

$$\eta \equiv -\frac{\ddot{H}}{2H\dot{H}} \ll 1. \tag{2.65}$$

In the slow-roll regime, the first Friedmann equation and the equation of motion, eqs. 2.56 and 2.55, simplify to

$$H^2 \simeq \frac{1}{3M_p^2}V, \tag{2.66}$$

$$3H\dot{\Pi} + V'(\Pi) \simeq 0. \tag{2.67}$$

Often it is convenient to work in terms of the potential, V, than in terms of Hubble parameters. We here define slow-roll parameters in terms of V as

$$\epsilon_v \equiv \frac{M_p^2}{2}\left(\frac{V'}{V}\right)^2 \ll 1, \tag{2.68}$$

and

$$\eta_v \equiv M_p^2\frac{V''}{V} \ll 1. \tag{2.69}$$

Note that ϵ_v corresponds to ϵ and η_v corresponds to $\epsilon + \eta$.

In the regime where the expansion of the universe is accelerated, we see that the slope and the curvature of the potential energy have to be small enough

Number of e-folds

Inflation must last for at least some duration of time to match the current observational data. Thus, we introduce a quantity called the number of e-folds denoted by N, defined as

$$N = \ln\frac{a_{end}}{a}, \tag{2.70}$$

where a_{end} is the scale factor at the end of the inflation. Since

$$dN = -d\ln a = -Hdt = -\frac{H}{\dot{\Pi}}d\Pi, \tag{2.71}$$

in the slow-roll regime, we can approximate N as [49]

$$N(\Pi) \simeq \int_{\Pi}^{\Pi_{end}} \frac{V(\tilde{\Pi})}{M_p^2 V'(\tilde{\Pi})}d\tilde{\Pi}. \tag{2.72}$$

Since the contribution from the curvature is defined as

$$\Omega_\kappa = -\frac{\kappa}{a^2 H^2}, \tag{2.73}$$

we have the relation from the onset of inflation to the end of the inflation

$$\Omega_k(a_{end}) \simeq \Omega(a_{in}) \frac{a_{in}^2}{a_{end}^2} \simeq e^{-2N}. \tag{2.74}$$

This relation tells us how the e-foldings and the contribution from the curvature is related. For example, if we had $\Omega_\kappa \sim 1$ at the beginning of inflation, after 20 e-foldings of inflation, we will have $\Omega_{\kappa,BBN} \sim 10^{-18}$.

From the observational data, we have the current total contribution, $\Omega_{tot}^{(0)} \equiv \Omega_{tot}(t_0) \simeq 1.02$. From the equation 2.31, we see that this observation means that there's no evident curvature [49]. Therefore, the curvature parameter, κ, throughout this thesis, is taken to be zero. From here on, when we refer to FLRW metric, we mean flat FLRW metric:

$$ds^2 = -dt^2 + a^2(t) d\vec{x}^2, \tag{2.75}$$

which can also be written as

$$ds^2 = a(\tau)^2[-d\tau^2 + d\vec{x}^2]. \tag{2.76}$$

Here, we introduced the conformal time, τ, with the relation $a(\tau)d\tau = dt$.

However, the universe is not completely homogeneous and isotropic. We have large scale structures such as galaxies and clusters of galaxies. In order to explain the formation of these large scale structures, we need to go beyond the homogeneity and isotropy approximation. The cosmological perturbation theory provides such a framework.

2.3 Cosmological Perturbation Theory

The theory of cosmological perturbations is the theory through which we understand how the quantum fluctuations during the very early universe can generate the seeds for the large-scale structures in the late time universe. This theory plays a very important role in the modern cosmology. In this section, the concept and the formulation of the theory will be explained. This discussion is mainly based on "Lectures on the Theory of Cosmological Perturbations" by Brandenberger [22] and "Theory of Cosmological Perturbations" by Mukhanov, Feldman, and Brandenberger [46].

2.3.1 Perturbative General Relativity

In the previous section, we introduced the FLRW metric with the line element

$$ds^2 = a(\tau)[-d\tau^2 + d\vec{x}^2], \tag{2.77}$$

as a background approximation to our universe on a cosmological scale. In this subsection, we introduce a formalism named after Arnowitt, Deser, and Misner: the ADM formalism [7]. The basic idea is that we can break down space-time into a foliation of 3-dimensional space-like manifold and a time direction. This formalism can be very useful when we work with perturbations. Using ADM formalism, we introduce three new quantities in the metric known as the lapse function, N, shift vector, N^i, and a 3-dimensional metric, h_{ij}. Using this formalism we can write the line element as

$$ds^2 = -N^2 d\tau^2 + h_{ij}(dx^i + N^i d\tau)(dx^j + N^j d\tau). \tag{2.78}$$

Note that for $N = a(\tau)$, $h_{ij} = a(t)^2\delta_{ij}$ and $N^j = 0$, this metric represents the flat FLRW metric.

To introduce inhomogeneities and anisotropies on top of the FLRW metric, we start by perturbing the ADM variables, N, N^i, and h_{ij}:

$$N = a(\tau)(1 + N_1) \tag{2.79}$$
$$N^i = \nabla^i\psi + N^i_T \tag{2.80}$$
$$h_{ij} = a(\tau)^2[(1 + 2\zeta)\delta_{ij} + 2E_{,ij} + F_{i,j} + F_{j,i} + \gamma_{ij}]. \tag{2.81}$$

Here, we separated perturbations into scalar (N_1, ψ, ζ, and E), vector (N^i_T and F_i), and tensor perturbations (γ_{ij}) by requiring

$$\begin{aligned} \nabla^i F_i = 0, \quad & \nabla_i N^i_T = 0 \\ \nabla^i \gamma_{ij} = 0, \quad & \gamma^i_i = 0. \end{aligned} \tag{2.82}$$

Here, ∇^i is a 3 dimensional covariant derivative from the 3 dimensional metric h_{ij}. Throughout this thesis, we will mostly study scalar perturbations.

Coordinate Transformation and Gauge Fixing

In the previous subsection, we introduced 7 variables to represent the metric perturbations. However, not all these variables correspond to actual degrees of freedom. Since the laws of

physics should not depend on the coordinates, we can use coordinate transformations to identify these artifacts. We start with a coordinate transformation

$$x^\mu \to x^\mu + \xi^\mu. \tag{2.83}$$

The spatial component ξ^i of ξ^μ can be decomposed into

$$\xi^i = \xi^i_\perp + h^{ij}\xi_{,j}, \tag{2.84}$$

where h^{ij} is the spatial background metric. The first term is a transverse part, which contributes to vector perturbations in the metric. The second term is the gradient of a scalar, which contributes to scalar perturbations [22].

If we just look at the scalar perturbations in eq. 2.79 - 2.81, we can see that these variables change under these coordinate transformation (eq. 2.83) as:

$$\begin{aligned} N_1 \to \tilde{N}_1 &= N_1 - \frac{a'}{a}\xi^0 - (\xi^0)' \\ \psi \to \tilde{\psi} &= \psi + \xi^0 - \xi' \\ E \to \tilde{E} &= E - \xi \\ \zeta \to \tilde{\zeta} &= \zeta + \frac{a'}{a}\xi^0, \end{aligned} \tag{2.85}$$

where primes denote derivatives with respect to τ, the conformal time. By choosing specific values of ξ^0 and ξ, we can fix the values of one or two of these variables. This formalism is referred as gauge fixing.

There are different gauges we can use for gauge fixing. For example, we can always take $\xi = E$, and $\xi^0 = E' - \psi$, such that in the new coordinate systems, the values of $E = \psi = 0$. This is the Newtonian or longitudinal gauge. In general, choosing a gauge will remove two degrees of freedom for scalar perturbations. As we will see later, these does not necessarily need to be E and ψ.

Similarly, the vector perturbations transform as

$$N^i_T \to \tilde{N}^i_T + \xi^{i\prime}_\perp, \qquad F_i \to \tilde{F}_i + \xi_{\perp i}. \tag{2.86}$$

Therefore, we can remove one vector perturbation variable through gauge fixing. From here on, we set $F_i = 0$.

Perturbations with Canonical Scalar Field

Many models of early universe, such as inflationary scenarios, involve scalar fields in the action. Therefore, in this subsection, we continue the discussion of metric perturbations in the context of a canonical scalar field minimally coupled to gravity. That represents the simplest model of generating scalar perturbations. The total action in this model can be written as

$$S = \frac{1}{2}\int d^4x\sqrt{-g}(\frac{1}{M_p^2}R - \partial_\alpha\Pi\partial^\alpha\Pi - 2V(\Pi)). \tag{2.87}$$

We can rewrite this action in terms of ADM variables and in conformal time as

$$S = \frac{1}{2}\int d^3x d\tau\sqrt{h}\left[NR^{(3)} - 2NV + N^{-1}(E_{ij}E^{ij} - E^2) + N^{-1}(\Pi' - N^i\partial_i\Pi)^2 - Nh^{ij}\partial_i\Pi\partial_j\Pi\right], \tag{2.88}$$

where $R^{(3)}$ is the 3 dimensional Ricci scalar, and E_{ij} and E given by

$$\begin{aligned} E_{ij} &\equiv \frac{1}{2}(h'_{ij} - \nabla_i N_j - \nabla_j N_i) \\ E &\equiv E^i{}_i. \end{aligned} \tag{2.89}$$

Here, h is the determinant of the spatial metric, h_{ij}.

In the previous subsection, we already derived perturbed ADM variables around the FLRW metric. We now need to take into account the fluctuations in the scalar field around the homogeneous background as well. We can represent this as

$$\Pi(\tau, \vec{x}) = \Pi_0(\tau) + \delta\Pi(\tau, \vec{x}). \tag{2.90}$$

We now have in total five variables corresponding to scalar perturbations ($\delta\Pi$, N_1, ψ, ζ, E). We can remove E by gauge fixing as mentioned earlier. However, note that under the transformation given in eq. 2.83, $\delta\Pi$ transforms as

$$\delta\Pi \to \delta\tilde{\Pi} - \Pi'_0\xi^0. \tag{2.91}$$

Therefore, through coordinate transformation, we can also remove $\delta\Pi$ instead of the other metric perturbation variable. This corresponds to choosing our time foliation along the Π constant hypersurfaces. This choice is known as the comoving gauge (or the Unitary gauge), which implies

$$\delta\Pi = 0, \quad h_{ij} = a(\tau)^2[(1 + 2\zeta)\delta_{ij} + \gamma_{ij}]. \tag{2.92}$$

The convenience of ADM formalism is that it makes it clear that the lapse function, and the shift vector are not dynamical variables. This allows us to remove two more degrees of freedom from the equation of motions for N, and N_i:

$$\nabla_i[N^{-1}(E^i_j - \delta^i_j E)] = 0 \tag{2.93}$$

$$R^{(3)} - 2V - N^{-2}(E_{ij}E^{ij} - E^2) - N^{-2}\Pi_0'^2 = 0. \tag{2.94}$$

These equations are referred to as Hamiltonian and momentum constraints. Solving these constraints, we find

$$N_1 = \frac{\zeta'}{\mathcal{H}}, \quad N^i_T = 0, \quad \nabla^2\psi = -\frac{1}{\mathcal{H}}\nabla^2\zeta + \frac{\Pi_0'^2}{2\mathcal{H}^2}\zeta', \tag{2.95}$$

where $\nabla^2 = \nabla_i\nabla^i = h^{ij}\nabla_i\nabla_j$.

We can plug these values in the action, given by eq. 2.87, along with the Friedmann equations for inflaton field to compute the part of the action which is second order in scalar perturbations

$$S_{(2)} = \frac{1}{2}\int d^3x d\tau\ a^2(\tau)\frac{\Pi_0'^2}{\mathcal{H}^2}[\zeta'^2 - (\partial_i\zeta\partial^i\zeta)], \tag{2.96}$$

where $\mathcal{H} \equiv a'/a$. The above equations reduces the analysis of scalar perturbations into the field theory of a single variable, ζ [22]. We often refer to ζ as the comoving curvature perturbation. This formulation allows us to apply techniques of quantum field theory in curved space-time to quantize cosmological perturbations.

2.3.2 Quantizing Cosmological Perturbations

To understand the generation of cosmological fluctuations, we need both Quantum Mechanics and General Relativity. Since universe is expanding, the wavelengths of fluctuations as we look into past gets smaller and smaller. In the context early universe scenarios, such as inflation, this implies that the fluctuations has to be treated as quantum fields. As long as gravity is weekly coupled, the theory of quantum field theory on curved space-time is sufficient to describe the quantum nature of fluctuations [22].

In previous sections, we showed that in an action described only by the gravitational term and a single scalar field, we can reduce the degrees of freedom to one single variable. Here, we show that trough a redefinition of variables, we can rewrite the action in a canonical form with a time dependent mass. This will lead to the production of quantum particles overtime.

Mukhanov Variable

As shown earlier, the Einstein-Hilbert term plus a scalar field $\Pi(t, \vec{x})$

$$S = \int d^4x\sqrt{-g}\left[\frac{1}{2M_p^2}R - \frac{1}{2}\partial_\mu\Pi\partial^\mu\Pi - V(\Pi)\right], \tag{2.97}$$

leads to the following quadratic action for the scalar perturbations:

$$S_{(2)} = \frac{1}{2}\int d^3x d\tau\ a^2(\tau)\frac{\Pi'^2}{\mathcal{H}^2}[\zeta'^2 - (\partial_i\zeta\partial^i\zeta)]. \tag{2.98}$$

The coefficient of the kinetic term in this action is time dependent. To resolve that we introduce v, known as the Mukhanov variable, given by

$$v = -z\zeta, \tag{2.99}$$

and

$$z = \frac{a\Pi_0'}{\mathcal{H}}. \tag{2.100}$$

In terms of these new variables, v and z, the quadratic action (eq. 2.98) becomes

$$S^{(2)} = \frac{1}{2}\int d^4x[v'^2 - v_{,i}v^{,i} + \frac{z''}{z}v^2]. \tag{2.101}$$

This equation represents the action of a single canonical field with a time-dependent mass.

The equation of motion for v is

$$v'' - \partial_i\partial^i v - \frac{z''}{z}v = 0. \tag{2.102}$$

In momentum space, the equation of motion becomes

$$v_k'' + k^2 v_k - \frac{z''}{z}v_k = 0. \tag{2.103}$$

With these equations, we can study how quantum fluctuations in early universe shaped the current cosmos, especially in inflationary scenarios.

Quantization and Initial Conditions

Since we derived the second order action

$$S = \frac{1}{2}\int d\tau\ d^3x\ \left[v'^2 - v_{,i}v^{,i} + \frac{z''}{z}v^2\right], \tag{2.104}$$

from eq. 2.97 in subsection 2.3.2, we can quantize the field in a standard way. First, we take the conjugate momenta of the field v,

$$\pi_v = \frac{\delta S}{\delta v'}, \tag{2.105}$$

which satisfies the commutation relation

$$[\hat{v}(\tau,\vec{x}), \hat{\pi}_v(\tau,\vec{x}')] = i\delta(\vec{x}-\vec{x}'), \tag{2.106}$$

and

$$[\hat{v}(\tau,\vec{x}), \hat{v}(\tau,\vec{x}')] = [\hat{\pi}_u(\tau,\vec{x}), \hat{\pi}_v(\tau,\vec{x}')] = 0. \tag{2.107}$$

Note that since the scalar field v has the canonical kinetic term, we have $\pi_v = v'$. Now, the quantum field v can be expanded in Fourier series:

$$\hat{v}(\tau,\vec{x}) = \frac{1}{\sqrt{(2\pi)^3}}\int d^3k \left\{\hat{a}_{\vec{k}} v_k(\tau)e^{i\vec{k}\cdot\vec{x}} + \hat{a}^\dagger_{\vec{k}} v^*_k(\tau)e^{-i\vec{k}\cdot\vec{x}}\right\}. \tag{2.108}$$

The operators, $a_{\vec{k}}$ and $a^\dagger_{\vec{k}}$ are the usual creator and annihilator operators, and the function v_k satisfying the usual classical equation of motion in Fourier space [49]. The normalization for the mode functions is given by

$$v_k v'^*_k - v^*_k v'_k = i. \tag{2.109}$$

Since we have quantized the fields, we turn our attention to the equation of motion:

$$v''_k + (k^2 - \frac{z''}{z})v_k = v''_k + (k^2 + m^2_{eff})u_k = 0. \tag{2.110}$$

As mentioned before, for the inflation to start, we need the slow-roll approximation. In the slow-roll regime, the evolution of $\dot{\Pi}$ and H is much smaller than the evolution of the scale factor, a (so we can see from the slow roll parameters $\ddot{\Pi}$ and $\dot{H}$ are much smaller than H). This means that we can approximate the effective mass as

$$m^2_{eff} = -\frac{z''}{z} \approx -\frac{a''}{a} = -\frac{2}{\tau^2}, \tag{2.111}$$

in de Sitter space-time. Note that as mentioned earlier, when $\rho \approx -P$, we have de Sitter space-time and exponentially increasing scale factor $a = e^{Ht}$. In this space-time, the equation for the conformal time

$$\tau = \int \frac{dt}{a} = \int e^{-Ht} dt = -\frac{1}{aH} \Rightarrow a \sim \frac{1}{H\tau}. \tag{2.112}$$

In de Sitter, and under the slow-roll regime, we have the general solution to the eq. 2.110 given by

$$v_k = \alpha e^{-ik\tau}\left(1 - \frac{i}{k\tau}\right) + \beta e^{ik\tau}\left(1 + \frac{i}{k\tau}\right). \tag{2.113}$$

In the region where the wavelength associated with a given k value is much less than the Hubble radius, we have $k|\tau| \gg 1$. Given, the normalization choice given by eq. 2.109, along with the requirement of Minkowski vacuum in that limit,

$$\lim_{\tau \to -\infty} v_k(\tau) = \frac{1}{\sqrt{2k}} e^{-k\tau}, \tag{2.114}$$

we obtain

$$v_k = \sqrt{\frac{1}{2k}} e^{-ik\tau}\left(1 - \frac{i}{k\tau}\right), \tag{2.115}$$

known as the *Bunch-Davis Vacuum* [41]. This vacuum state is a zero particle state in the asymptotic past infinity.

Power Spectrum and Two Point Correlation Function

The power spectrum P_v of the quantum fluctuations v is given by

$$P_v(k) = k^3 |\tilde{v}(k)|^2, \tag{2.116}$$

where $\tilde{v}(k)$ is from the Fourier transformation

$$\tilde{v}(\vec{k}, t) = \int d^3x v(\vec{x}, t) e^{-i\vec{k}\cdot\vec{x}}. \tag{2.117}$$

We can define the correlation function for the scalar field v, which gives us the relation

$$\langle 0 \left| \hat{v}(\vec{x}_1)\hat{v}(\vec{x}_2) \right| 0 \rangle = \int d^3k \; e^{i\vec{k}\cdot(\vec{x}_1 - \vec{x}_2)} \frac{P_v(k)}{4\pi k^3}, \tag{2.118}$$

where P_v is the power spectrum for the scalar field v [41]. Since $v = -z\zeta$, the power spectrum of the curvature perturbation ζ becomes

$$P_\zeta = k^3|\zeta_k|^2, = k^3\frac{|v_k|^2}{z^2} = \frac{P_v}{z^2} \tag{2.119}$$

since $\zeta = z^{-1}v$. In the region where the wavelength is smaller than the Hubble radius ($k|\tau| \gg 1$), we have

$$P_\zeta(k) \simeq \frac{H^2}{4k^3\epsilon}, \tag{2.120}$$

where $\epsilon = \dot{\Pi}^2/H^2$. From the CMB data we obtain the amplitude of the primordial power spectrum to be $P_v^{1/2} \simeq 5\times10^{-5}$. We can write the power spectrum in terms of the potential and the slow-roll parameter (2.68)

$$P_\zeta = \frac{1}{24\pi^2}\left(\frac{V}{M_p^4\epsilon_v}\right). \tag{2.121}$$

This equation now gives us the restriction on the energy scale during inflation. For example, if $\epsilon_v \sim 1$ then we get

$$V^{1/4} \sim 10^{-3} \sim 10^{15}\ \text{GeV}. \tag{2.122}$$

2.3.3 Summary

In this chapter, we started by introducing the most accepted mathematical theory for describing gravity, the General Theory of Relativity. We showed how this theory allows us to understand the background evolution of the universe, and how the components of matter in the universe can contribute to the evolution. We proceeded to introduce the Hot Big Bang model, which had its successes but also had many puzzles, such as the horizon problem. Then we introduced a possible solution: inflation - the accelerated expansion of the universe at early times. We explained how it could solve the horizon and flatness problems, and how the background would evolve in this model. We then introduced inhomogeneities in our picture, and quantized these perturbations, and how they could generate the observed power spectrum.

This chapter's purpose was to expose to readers the essential frameworks and models to understand the rest of the thesis, which focuses on exploring the limitations of the current paradigm of cosmology (the standard inflationary Big Bang model). For example, we do not quite know what the initial condition for the beginning of the universe. It seems that

assuming Bunch Davies initial conditions gives us nice predictions, but there are debates on the validity of this assumption. Another famous problem in the field of cosmology is the cosmological constant problem, where we cannot reconcile predictions from quantum field theories and general relativity. The next chapters will look to these puzzles in inflationary Big Bang scenarios by suggesting alternative models, or using techniques such as effective field theories.

Chapter 3

Cuscuton: IR Modification of Gravity

To answer some of the problems in the standard inflationary Big Bang model, many methods and approaches have been made, with interesting models. In this chapter, we introduce a causal scalar field theory with non-canonical kinetic terms called Cuscuton, a Latin name of a parasitic plant of dodder [3]. The field gets its name because it becomes an auxiliary field, and follows the dynamics of the field that it attaches or couples to [3]. Since its first proposal, the cuscuton has been seen in many independent works in cosmology/high-energy physics. The low energy limit of Horava gravity[35], the different types of inflationary models [20], approaches to resolve cosmological constant [28] are some of the examples of where we can see the rediscovery of cuscuton.

In this chapter, we will study the second order action of cuscuton based on the works of Boruah et al. [21]. Although there were many works regarding cuscuton cosmology, the second order action of cuscuton in terms of the curvature perturbation ζ had not been obtained. This is a significant step forward because with the obtained second order action for ζ, we can rigorously explore the evolution of its fluctuations. In this chapter, we will begin by a brief review of cuscuton, then we will obtain the second order action in terms of ζ and background quantities and present the analysis of the result. Finally, we will conclude the chapter by commenting on the analysis and the possible future works.

3.1 Introduction

To conjure such field consider an action given by

$$S = \int d^3x d\tau \, \sqrt{-g} \, [P(X, \varphi)] \, , \tag{3.1}$$

where τ is the conformal time, and X given by $X = \partial_\mu \varphi \partial^\mu \varphi$, and φ is a scalar field. In a homogeneous and isotropic background with metric

$$ds^2 = a^2(\tau)(-d\tau^2 + \delta_{ij} dx^i dx^j), \tag{3.2}$$

the equation of motion of such field takes the following form [21]

$$(P_{,X} + 2X P_{,XX})\varphi'' + 3\mathcal{H} P_{,X}\varphi' + P_{,X\varphi}\varphi'^2 - \frac{1}{a^2} P_{,\varphi} = 0. \tag{3.3}$$

Again, $P_{,X}$ denotes the partial derivative of P with respect to X. For the second derivative terms to vanish, it requires that [3] [21]

$$(P_{,X} + 2X P_{,XX}) = 0. \tag{3.4}$$

A theory where the above condition is automatically satisfied is

$$S = \int d^4x \sqrt{-g} [\pm \mu^2 \sqrt{X} - V(\varphi)]. \tag{3.5}$$

The equation of motion for this theory at all orders in perturbations is given by

$$\left(g_{\mu\nu} - \frac{\partial_\mu \varphi \partial_\nu \varphi}{X} \right) \nabla^\mu \nabla^\nu \varphi \pm \frac{1}{\mu^2} \sqrt{X} V'(\varphi) = 0. \tag{3.6}$$

By doing a simple analysis of the above equation at zeroth order of perturbation, we can see that the above equation will lead to no second order derivatives. However, even at the first order of perturbation, the second order derivative terms vanish.

We now develop the cosmological perturbation theory for this theory. We will also show that the scalar comoving curvature perturbation ζ is conserved in super-horizon scales in the frameworks of cuscuton gravity and that the cuscuton theory is ghost free.

3.2 Background Cosmology with Cuscuton

Since the cuscuton field is an auxiliary field and lacks its own dynamics, we need another field with propagating degrees of freedom to study the dynamics of the cuscuton field. To do that, we will consider a scalar field Π with a canonical kinetic term and minimally coupled to cuscuton to be the source of the scalar mode. Then, we have the action

$$S = \int d^4x\sqrt{-g}\left[\frac{1}{2}R - \frac{1}{2}\partial_\mu\Pi\partial^\mu\Pi - U(\Pi) \pm \mu^2\sqrt{-\partial_\mu\varphi\partial^\mu\varphi} - V(\varphi)\right]. \tag{3.7}$$

Now from the eq. 2.22, and the Einstein field equations, we can get two background equations

$$3\mathcal{H}^2 = \frac{1}{2}\Pi_0'^2 + V(\varphi_0)a^2 + U(\Pi_0)a^2 \tag{3.8}$$

$$\mathcal{H}^2 - \mathcal{H}' = \frac{1}{2}\Pi_0'^2 \pm \frac{\mu^2}{2}|\varphi_0'|a, \tag{3.9}$$

where the subscript 0 denotes the back ground homogeneous quantities. The above two equations give us two constraints on background parameters. Note that the right hand side of eq. 3.9 gives $\mathcal{H}^2 - \mathcal{H}' = -\dot{H}a^2$. Then we have a relation

$$\dot{H} = -\frac{1}{2a^2}\Pi_0'^2 \mp \frac{\mu^2}{2a}|\varphi_0'|. \tag{3.10}$$

Interestingly, we notice if we choose the negative sign choice for the sign of μ^2 term in the action, it allows us to have a positive value for $\dot{H}$.In standard GR positive $\dot{H}$ would require $-\Pi_0'^2$ for kinetic term and would violate the Null Energy Condition. However, here the sign of the $\Pi_0'^2$ does not need to change, and thus the Null Energy Condition for the source scalar field is not violated even with $\dot{H} > 0$. Thus, we do not expect any ghost instabilities, and later in the chapter, we will show that this is true.

Also, by defining two parameters

$$\alpha \equiv \frac{\Pi_0'^2}{2\mathcal{H}^2} \tag{3.11}$$

$$\epsilon \equiv \frac{\mathcal{H}^2 - \mathcal{H}'}{\mathcal{H}^2}, \tag{3.12}$$

we can write the cuscuton contribution on the background equations as a new parameter:

$$\sigma \equiv \epsilon - \alpha = \pm\frac{\mu^2}{2\mathcal{H}^2}|\varphi_0'|a. \tag{3.13}$$

Note that in the limit $\mu^2 \to 0$, we get $\sigma \to 0$. In the standard inflationary model, α equals to ϵ, and its value represents the the first slow roll parameter introduced in eq. 2.68 [21].

The equation of motion for cuscuton (3.6) at zeroth order in perturbations reduces to

$$\pm 3\mu^2 \,\mathrm{sign}\,(\varphi_0')\mathcal{H} = -aV_{,\varphi}(\varphi_0). \tag{3.14}$$

For a specific potential we can write φ as

$$\varphi_0 = V_{,\varphi}^{-1}\left(\mp\frac{3\mu^2\,\mathrm{sign}(\varphi_0')\mathcal{H}}{a}\right). \tag{3.15}$$

Thus, the eq. 3.8 can be written as

$$3\mathcal{H}^2 = \frac{1}{2}\Pi_0'^2 + U(\Pi_0)a^2 + V\left(V_{,\varphi}^{-1}\left(\mp\frac{3\mu^2\,\mathrm{sign}(\varphi_0')\mathcal{H}}{a}\right)\right)a^2, \tag{3.16}$$

which shows how Friedmann equation gets modified due to cuscuton correction to GR.

Finally, we have one more background equation from the equation of motion of the scalar field Π,

$$\Pi_0'' + 2\mathcal{H}\Pi_0' - a^2\frac{\partial U}{\partial \Pi}\Pi_0' = 0. \tag{3.17}$$

However, this is a dynamical equation and therefore does not act as a constraint equation.

3.3 Curvature Perturbations with Cuscuton

In this section, we turn our attention to linear perturbations of scalar fields and the metric. We first write the metric with ADM variables, which provide a convenient way of splitting space-time into a 3-dimensional space-like hypersurface and a time direction [21][7]. The metric in ADM variables is written as

$$ds^2 = -N^2 d\tau^2 + h_{ij}(dx^i + N^i d\tau)(dx^j + N^j d\tau), \tag{3.18}$$

where N is the lapse, N^j is the shift, and h_{ij} is the metric of the 3-dimensional hypersurface given by

$$h_{ij} = a^2[(1+\zeta)\delta_{ij} + \gamma_{ij}]. \tag{3.19}$$

The scalar parameter ζ is also known as the comoving curvature perturbation in the standard inflationary scenario. The tensor parameter γ_{ij} is the traceless, gradientless($\gamma_i^i = 0$, $\partial^i\gamma_{ij} = 0$) part of the 3-dimensional metric.

With the ADM formalism we can write the total action in terms of ADM variables. The Einstein-Hilbert action, the action with canonical scalar field, and the cuscuton action can be re-written as

$$S_{EH} = \frac{1}{2}\int d^3x d\tau \sqrt{-g}R = \frac{1}{2}\int d\tau d^3x \sqrt{h}\left[NR^{(3)} + N^{-1}(E_{ij}E^{ij} - E^2)\right]. \tag{3.20}$$

$$S_\Pi = \frac{1}{2}\int d\tau d^3x \sqrt{h}\left[N^{-1}(\Pi' - N^i\partial_i\Pi)^2 - Nh^{ij}\partial_i\Pi\partial^j\Pi - 2NU(\Pi)\right]. \tag{3.21}$$

$$S_\varphi = \frac{1}{2}\int d\tau d^3x \sqrt{h}\left[\pm 2\mu^2\sqrt{((\varphi' - N^i\partial_i\varphi)^2 - N^2h^{ij}\partial_i\varphi\partial_j\varphi)} - 2NV(\varphi)\right], \tag{3.22}$$

where $R^{(3)}$ is the Ricci scalar of the hypersurface, $\sqrt{h}$ is the square root of the determinant of the 3-dimensional metric h_{ij} and

$$E_{ij} = \frac{1}{2}h'_{ij} - \frac{1}{2}(\nabla_i N_j + \nabla_j N_i) \quad \text{and} \quad E = E^i{}_i. \tag{3.23}$$

Variation of the total action $S_{EH} + S_\Pi + S_\varphi$ with respect to lapse and shift gives us the momentum and Hamiltonian constraints,

$$\nabla_i(N^{-1}(E^i{}_j - \delta^i_j E)) = q_{,j} \tag{3.24}$$

$$R^{(3)} + N^{-2}(E^2 - E^{ij}E_{ij}) = 2\rho, \tag{3.25}$$

where $q_{,i}$ and ρ are the momentum density and the total energy density respectively.

The scalar perturbations give us two gauge degrees of freedom. We can fix one degree of freedom by choosing a comoving uniform field gauge with respect to Π field such that $\delta\Pi = 0$. Another freedom can be fixed by setting

$$\gamma_{ij} = 0, \tag{3.26}$$

such that

$$h_{ij} = a^2(1 + 2\zeta)\delta_{ij}. \tag{3.27}$$

The scalar contributions to N and N_i can be written as [21]

$$N_i = \nabla_i\psi \qquad N = a(1 + N_1). \tag{3.28}$$

The constraint equation, eqs. 3.24 and 3.25, give us

$$N_1 = \frac{\zeta'}{\mathcal{H}} \pm \frac{1}{2}\mu^2 a\,\mathrm{sign}(\varphi'_0)\frac{\delta\varphi}{\mathcal{H}} \tag{3.29}$$

$$\nabla^2\psi = -\frac{1}{\mathcal{H}}\nabla^2\zeta + \frac{\Pi'^2_0}{2\mathcal{H}}N_1. \tag{3.30}$$

Notice that with metric and scalar field perturbations, we had six perturbative variables, N_1, ψ, ζ, $\delta\varphi$, $\delta\Pi$, and γ_{ij}. We removed two degrees of freedom by fixing $\delta\Pi = 0$, and $\gamma_{ij} = 0$. We also fixed two more freedom by eq. 3.29 and 3.30, fixing N_1, and ψ in terms of other variables. Now we can write the action to the second order in perturbation in terms of only ζ and $\delta\varphi$:

$$\begin{aligned} S^{(2)}_{EH} &= \int d\tau d^3x\, a^2 \left\{ \left[\frac{3\epsilon}{2} - 9\right](\zeta\mathcal{H})^2 - \epsilon(\partial\zeta)^2 + \mu^2 a\delta\varphi \left[\alpha\zeta' - \frac{9}{2}\zeta\mathcal{H}\right] \right. \\ &\qquad \left. -(\mu^2 a\delta\varphi)^2 \left[\frac{\alpha}{2} + \frac{3}{4}\right]\right\} \qquad (3.31) \\ S^{(2)}_{\varphi} &= \int d\tau d^3x\, a^2 \left\{ \left[6(\alpha-\epsilon) + \left[\frac{3Va^2}{\mathcal{H}^2}\right]\left(1+\frac{\epsilon}{2}\right)\right](\zeta\mathcal{H})^2 + \mu^2 a\delta\varphi \left[\frac{3a^2V}{2\mathcal{H}^2}(\zeta\mathcal{H}) \right.\right. \\ &\qquad \left.\left. -\frac{1}{2}\alpha\zeta' + \frac{\partial^2\zeta}{2\mathcal{H}}\right] + (\mu^2 a\delta\varphi)^2\left(\frac{\alpha}{4}+\frac{3}{4}\right)\right\} \qquad (3.32) \\ S^{(2)}_{\Pi} &= \int d\tau d^3x\, a^2 \left\{ \alpha\zeta'^2 + \left[\left(9 - 6\alpha + \frac{9\epsilon}{2}\right) - \frac{3Va^2}{\mathcal{H}^2}\left(1+\frac{\epsilon}{2}\right)\right](\zeta\mathcal{H})^2 \right. \\ &\qquad \left. +\mu^2 a\delta\varphi\left[\left(\frac{9}{2} - \frac{3a^2V}{2\mathcal{H}^2}\right)\zeta\mathcal{H} - \alpha\zeta'\right] + \frac{1}{4}(\mu^2 a\delta\varphi)^2\right\} \qquad (3.33) \end{aligned}$$

Combining these expressions we obtain the expression ,

$$S^{(2)} = \int d\tau d^3x\, a^2 \left[\alpha\zeta'^2 - \epsilon(\partial\zeta)^2 + \sigma\left(\frac{\mathcal{H}\delta\varphi}{\varphi_0'}\right)\left(\alpha\mathcal{H}\zeta' - \partial^2\zeta\right)\right] . \qquad (3.34)$$

In the limit where $\sigma \to 0$, we can see that the contributions from cuscuton vanish and the above action eq. 3.34 simplifies to

$$S^{(2)} = \int d\tau d^3x\, a^2 \left[\alpha\zeta'^2 - \epsilon(\partial\zeta)^2\right] = \int d\tau d^3x\, a^2\alpha \left[\zeta'^2 - (\partial\zeta)^2\right], \qquad (3.35)$$

which is the standard quadratic action for curvature perturbations [21].

The total action is now written with only two perturbation variables, ζ and $\delta\varphi$. We can remove one more variable using the field equation for cuscuton as a constraint equation:

$$\nabla^2\delta\varphi - \mathcal{H}^2\alpha[3+\alpha-\epsilon]\delta\varphi = \frac{\varphi_0'}{\mathcal{H}}[\nabla^2\zeta - \alpha\mathcal{H}\zeta']. \qquad (3.36)$$

However, to write $\delta\varphi$ in terms of other variables, we need to invert derivative opvaertors. Thus, we will begin working in fourier space and then we can write $\delta\varphi$ in fourier space as

$$\delta\varphi_k = \frac{\varphi_0'}{\mathcal{H}} \frac{\mathbf{k}^2\zeta_k + \alpha\mathcal{H}\zeta_k'}{[\mathbf{k}^2 + (3+\alpha-\epsilon)\alpha\mathcal{H}^2]}. \tag{3.37}$$

We can now write eq. 3.34 as

$$S^{(2)} = \int d\tau d^3k \; z^2 \left[\zeta_k' - c_s^2\mathbf{k}^2\zeta_k^2\right]. \tag{3.38}$$

Here, we introduced two functions $z(\mathbf{k},\tau)$ and $c_s(\mathbf{k},\tau)$ given by

$$z^2 \equiv a^2\alpha \left(\frac{\mathbf{k}^2 + 3\alpha\mathcal{H}^2}{\mathbf{k}^2 + \alpha\mathcal{H}^2(3-\sigma)}\right) \tag{3.39}$$

$$c_s^2 \equiv \frac{\mathbf{k}^4 + \mathbf{k}^2\mathcal{H}^2\mathcal{B}_1 + \mathcal{H}^4\mathcal{B}_2}{\mathbf{k}^4 + \mathbf{k}^2\mathcal{H}^2\mathcal{A}_1 + \mathcal{H}^4\mathcal{A}_2}, \tag{3.40}$$

where we also introduce some other notations given by

$$\eta \equiv \frac{\epsilon'}{\mathcal{H}\epsilon} \tag{3.41}$$

$$\beta \equiv \frac{\alpha'}{\mathcal{H}\alpha} \tag{3.42}$$

$$\mathcal{A}_1 \equiv 6\alpha - \alpha\sigma \tag{3.43}$$

$$\mathcal{A}_2 \equiv 9\alpha^2 - 3\alpha^2\sigma \tag{3.44}$$

$$\mathcal{B}_1 \equiv \mathcal{A}_1 + \sigma(6+\eta+\beta+2\epsilon) + \alpha(\eta-\beta) \tag{3.45}$$

$$\mathcal{B}_2 \equiv \mathcal{A}_2 + \sigma\alpha(12 - 4\sigma + 3\eta) + 3\alpha^2(\eta-\beta). \tag{3.46}$$

Note that in the $\sigma \to 0$ limit, we get $c_S^2 \to 1$ and $z^2 \to a^2\alpha$ as expected for the case of the standard scalar field. Also, we see that the same is true for the ultra-violet case where $k \to \infty$.

3.4 Analysis

Ghosts

When a field has the wrong sign of the kinetic term, we refer to this as ghosts. If the kinetic term has a negative sign, as the field vibrates more, we get a negative energy unbounded

below. The vacuum state, which is the lowest energy state, will be unbounded below, and any system will roll towards the infinite negative energy state. This instability is why we do not want ghosts in our theory.

In the ultra-violet limit of the theory, the coefficient of the ζ'^2 term is $z^2 \sim a^2\alpha > 0$, which implies that the theory is ghost free independent of ϵ or the sign choice for μ^2 in the action [21]. In fact, if we choose a negative sign for μ^2, the sign of σ will always be negative and we will not have any ghosts. Although for the positive sign of μ^2, the sign of z^2 can change depending on the value of σ as can be seen in the eq. 3.39, the notion of ghost instabilities is only meaningful in the ultra-violet limit and we do not need to worry about ghosts [21]. When we deviate from the limit of flat background or time independent actions, energy conservation and plain wave description of modes breaks down. The Hamiltonian could become negative, but that does not necessarily mean instabilities within the system. In fact, during the standard inflationary scenario, the Hamiltonian becomes negative in on super horizon scales and resembles excited states with negative energy, but the theory is still healthy.

Other Instabilities and Poles

Although the theory does not have ghosts, we might have other issues such as gradient instability. Whether a scenario shows instability or not depends on the parameters of the model.

To study possibilities of instabilities, consider the equation of motion for ζ_k from the action (3.34)

$$\zeta_k'' + \left(2 + \beta + \frac{\mathcal{C}_1\mathcal{H}^2\mathbf{k}^2 + \mathcal{C}_2\mathcal{H}^4}{\mathbf{k}^4 + \mathbf{k}^2\mathcal{H}^2\mathcal{A}_1 + \mathcal{H}^4\mathcal{A}_2}\right)\mathcal{H}\zeta_k' + c_s^2\mathbf{k}^2\zeta_k = 0, \tag{3.47}$$

where

$$\mathcal{C}_1 = (\beta + 2\alpha - 2\alpha^2 - 2\alpha\sigma)\sigma + 3\alpha^2(\eta - \beta) \tag{3.48}$$

$$\mathcal{C}_2 = 3\alpha^2(\eta - \beta). \tag{3.49}$$

As we see there are quite a few parameters that can determine the sign and behaviour of c_s^2 and coefficients of ζ_k'. While we can not make conclusive statement for every cuscuton scenario, we comment on some generic features. First, in UV limit all the cuscuton contributions go away and $c_s^2 \to 1$. Therefore, there is no gradient instability in that limit.

Second, the non trivial denominator shared in one of the coefficients of ζ_k' and c_s^2 can be factored as

$$\mathbf{k}^4 + \mathbf{k}^2\mathcal{H}^2\mathcal{A}_1 + \mathcal{H}^4\mathcal{A}_2 = (\mathbf{k}^2 + 3\alpha\mathcal{H}^2)(\mathbf{k}^2 + \alpha\mathcal{H}^2(3-\sigma)). \tag{3.50}$$

Therefore, for $-\mu^2$ in the action or $+\mu^2$ with $\sigma < 3$, the equation of motion for ζ_k is not singular. Models with $+\mu^2$ and $\sigma \geq 3$ can allow for poles which make the equation of motion for ζ_k singular. Singular ODEs are not necessarily catastrophic and they may be treatable. In fact as we mentioned before for $+\mu^2$, eq. 3.13, dictates that $\epsilon > 0$ at all times. Therefore, an expanding universe can not go through a bounce. It turns out for $+\mu^2$ and $\epsilon > 0$, one can write the equation of motion for Φ potential in longitudinal gauge and there the equation is not even singular [2].

Conservation for ζ

Now we see if the parameter ζ_k is conserved in the infrared limit where $k \to 0$. In this limit, given that $\sigma \neq 3$, $z^2c_s^2$ becomes finite and the equation of motion can be approximated to

$$\frac{d}{d\tau} z^2 \zeta_k' \approx 0. \tag{3.51}$$

The solutions to this will have a constant mode for ζ_k and a time dependent mode that goes like $\int d\tau/z^2$ [21]. Then using eq. 3.39, and defining the number of e-fodling as $N \equiv \ln a$, we get

$$\zeta_{IR}^{(time)} \propto \int \frac{d\tau}{z^2}\bigg|_{IR} \approx \int \left(\frac{1-\frac{\sigma}{3}}{\alpha}\right)\left(\frac{dN}{e^{3N} - \int \epsilon d\tilde{N}}\right). \tag{3.52}$$

This shows that, in an expanding universe where N is increasing in time, $\epsilon < 3$ can lead to a decaying mode beyond the horizon, but $\epsilon \geq 3$ can give us a growing mode. Also, we can expect the opposite case for the decreasing N case (contracting universe) [21].

ζ Comparisons

We now turn our attention to how our ζ differs from other definitions of ζ in other literature. In single field models, ζ_s sometimes is defined as

$$\zeta_s = \Phi + \frac{\Phi' + \mathcal{H}\Phi}{\epsilon\mathcal{H}} \tag{3.53}$$

in Newtonian guage. By performing time transformation $t \to t - \psi$, we can see that our ζ and ζ_s are related by the relation

$$\zeta_s = \zeta - \frac{\sigma \mathcal{H} \delta\varphi}{\varphi_0'}. \tag{3.54}$$

Using the definiton given by eq. 3.37 and working in Fourier space, we get

$$\zeta_k = \Phi_k + \frac{\Phi_k' + \mathcal{H}\Phi_k}{\epsilon \mathcal{H}} \left[1 - \frac{3\mathcal{H}^2\sigma}{\mathbf{k}^2 + 3\mathcal{H}^2\epsilon} \right]. \tag{3.55}$$

Note that in the ultra-violet and in $\sigma \to 0$ limit, this matches with eq. 3.53. In the infrared limit, we have

$$\zeta_s \simeq \zeta + \frac{\sigma}{\mathcal{H}(3-\sigma)} \zeta'. \tag{3.56}$$

We can see that if ζ is conserved ζ_s is also conserved.

3.5 Summary and Future Works

The main goal of this work was to obtain the quadratic action for comoving curvature perturbations, ζ, in cuscuton models. We started from an action that included the standard Hilbert-Einstein term, a canonical scalar field and a cuscuton field. We then used ADM formalism and the uniform field gauge with respect to the scalar field to obtain the quadratic action for ζ. In order to eliminate the cuscuton dependence from this action we had to invert the cuscuton constraint equation. Therefore, we carried on the derivation in Fourier Space. As we expected our final action eq. 3.38 had a complicated form but it explicitly shows that cuscuton models are ghost free and have no instabilities in UV limit. Basically in UV limit, the action becomes the standard quadratic action for a scalar field, minimally coupled to gravity. Upon further investigation of equation of motion for ζ_k in section 3.4, we also saw that there are no out of ordinary instabilities on non-UV scales either. This analysis shows that depending on the details of a particular cuscuton model and the potential of the scalar field, some corners of parameter space may lead to growing modes. Interestingly, it seems if we choose a $-\mu^2$ for cuscuton kinetic term in the action, there is more flexibilities in engineering different background evolutions and less chance of developing instabilities. That will be very useful in engineering bounce scenarios. In order to get a bounce one has to choose $-\mu^2$ in the action and make the parameter ϵ become negative. However, with cuscuton that does not lead to ghosts since the source field does not violate null energy condition. This could be the subject of our possible next upcoming

project. We also showed that our choice of ζ was consistent with producing a conserved mode on super horizon scales. However, we noticed that other common definitions of ζ while are different physical quantities, they also produce a conserved mode and all of these definitions merge on small scales. From computation point, we found that derivation of equations and action were considerable simpler when we picked ζ as the comoving curvature perturbation with respect to the source field.

For possible future works following the analysis of second order action with cuscuton, we could study a possible bounce scenario in the early universe. To properly study the bounce case with cuscuton, we will need to study the equation of motion for ζ and see how it evolves over time. Furthermore, we will need to specify the potential $V(\varphi_0)$, and see how parameters, such as $a(\tau)$, H, $\dot{H}$ behaves. The next course for this field should involve setting a toy model, an initial condition and studying the differential equation to see how ζ behaves over time.

Chapter 4

Effective Field Theory and Modified Dispersion Relations

The standard Big Bang model with inflation poses the trans-Planckian problem, and we do not know if Bunch-Davies initial condition is suitable. However, even with the absence of high energy physics at such scales, we can still construct a systemic way to make progress. In this chapter, we will show the technique of effective field theory(EFT) in the inflationary picture, and how this could give us modified dispersion relations that leads to a modification to the Bunch-Davies initial conditions.

4.1 Introduction

Much has been said and written about the possible effects due to perturbation modes evolving inside the horizon with energies larger than the scale of known physics (see Refs. [44, 30, 32, 29, 31, 38, 39, 40, 24, 9, 10, 8, 6] for a few examples). Depending on how one models the new physics, various assessments for the amplitude of the corrections to standard quantum field theory results were suggested. In fact, in most scenarios, these effects were estimated to be of order $(H/M)^n$, where H and M are respectively the inflationary Hubble parameter and scale of new physics, and the exponent $n \gtrsim 1$, typically.

One approach to model physics at very high momenta, is to assume that the Lorentzian dispersion relation, $\omega^2 = k^2$, is modified by higher order corrections. Depending on whether the dispersion relation respects the adiabaticity condition when the mode are inside the horizon, the corrections to the spectrum can be negligible [45] or dominant [43, 55]. The

authors of these studies used the gluing approximation to estimate the corrections. However, comparing the outcome of this approximation in the case of Ref. [45] with the exact analytical solution, authors of [13] showed that the gluing method overestimates the correction to the power spectrum by an extra factor of (H/M). Moreover, for a dispersion relation with non-adiabatic evolution, the numerical solution for the mode equation suggests that the effect is drastically different from what the gluing technique predicts. In Ref. [43], the gluing method indicated that the correction to the power spectrum is given by an oscillatory function whose amplitude depends almost linearly on the amount of time each mode spends in the non-adiabatic region. The numerical solution on the other hand demonstrated that the exact behaviour of the power spectrum is more involved, depending on other parameters in the problem [36]. It is often argued that effects of order one or higher on the power spectrum (see [51] as an example) should be excluded due to the back-reaction of excited states in the phase governed by the known physics [54]. However, as demonstrated in Ref. [33], as long as the scale of new physics is different from the Planck scale, the back reaction is not very constraining for corrections to observables like the power spectrum. They estimated the upper bound on the second Bogolyubov coefficient to be of order $\sqrt{\varepsilon\,\eta}\,H\,M_{\rm p}/M^2$, where ε and η are respectively the first and second slow-roll parameter for a given inflationary potential and $M_{\rm pl}$ is the Planck mass. In fact, for a given inflationary model, the back reaction of excited states with large Bogolyubov coefficients, could be counteracted by simultaneously reducing the ratio of H and M [15]. Further more, for a large-field model of inflation with highly excited initial condition the new physics scale cannot be arbitrarily larger than the Hubble parameter during inflation [15]. For example for the quadratic potential, the largest value allowed turns out to be $M \simeq 21\,H$. In this thesis, we call such highly excited initial conditions as "super-excited" states. These super-excited initial conditions can generate interesting observational effects. For instance, super-excited states with k dependence, induce a running in the spectral index larger than $\mathcal{O}(\epsilon^2)$ [14]. In another example, it was shown that the position-dependent modulations of excited states with large occupation numbers lead to the hemispherical anomaly [1]. In a recent work, the effect of rotational symmetry-breaking excited initial conditions was used to obtain statistically anisotropic power and bi-spectrum. Such an effect is not yet observed in the CMB, but may have an impact for future galaxy surveys, leaving a trace in the shape of galaxies [26].

All of the above motivates us to further investigate the microphysical origin of such super-excited initial states. Recalling that dispersion relations with an intermediate phase that break WKB condition can induce large corrections to the power spectrum, we were inspired to further study the implications of modified dispersion relations for excited initial states. In particular, we are exploring the modified dispersion relations of the following

form

$$\omega^2(k_{\rm ph}) = \bar{\beta}\, k_{\rm ph}^6 - \bar{\alpha} k_{\rm ph}^4 + k_{\rm ph}^2 \ , \tag{4.1}$$

where $\bar{\beta}$, $\bar{\alpha} \geq 0$. In particular, we like to explicitly show that the region of parameter space that results in larger than one modification of the power spectrum corresponds to an initial condition with super excited state in standard picture. To estimate the solution of the mode equation, we use both the analytical technique called gluing as well as numerical techniques. Gluing method has been used quite extensively in the literature [45] for estimating the power spectrum. In this method, the solution to the differential equation in different regions of the domain are glued to each other by matching the functions and their first derivatives at the boundaries. The initial condition is usually set to be adiabatic vacuum which corresponds to positive frequency WKB mode at infinite past. However, one has to keep in mind that the precision of this method relies strongly on how well the solutions overlap or merge at the boundaries. In the case of $\bar{\beta} = 0$ and $\bar{\alpha} < 0$, we have an exact analytic solution for mode equation (4.1), and therefore we can extract the *exact* correspondence to Bogolyubov coefficients. This allows us to test the reliability of the gluing prediction in this case. As we will show the second Bogolyubov coefficient goes to zero much faster than what the simple matching technique suggests. The discrepancy between the two methods can be as significant as order $(H/M)^2$.

For $\bar{\beta} \neq 0$ and $\bar{\alpha} > 0$, one has a sixth order polynomial dispersion relation with an intermediate phase that dispersion curve has negative slope. In this case no exact analytic solution is known for equation of motion (4.1). However, matching excited mode solutions to the implicit solution given by Mathematica will provide us the corresponding Bogolyubov coefficients. In our approach, we make sure that the matching is performed in the regime that solutions are overlapping to a high precision. As we will observe, these dispersion relation even in the cases where there is only one turning point in the equation (corresponding to usual Hubble crossing) can mimic excited states with particle number density as large as 80. This verifies the result of previous studies [14, 16, 12]. Our derivation also shows that in some regions of parameter space, above dispersion relation does not lead to any corrections to power spectrum. We will identify the corresponding "calm excited states" [17] resulting from the evolution of these modes. In the last section, we will comment on how dispersion relations like the one in Eq. (4.1) can arise in the context of the Effective Field Theory of Inflation [25]. Finally, we will present a conclusion and propose avenues for future developments.

4.2 Precision of gluing method for estimating power spectrum

As already pointed out, we want to study the effects of modified dispersion relations on the power spectrum. Modified dispersion relations can lead to complicated Ordinary Differential Equations (ODEs) in Fourier space that are hard to solve analytically. A popular analytical method in the literature to estimate the solution of an ODEs, is to use matching techniques. In this approach, one first finds the general solutions to the ODE in different domains. Imposing an initial or boundary condition then fixes the coefficients in one region, and the coefficients in the other regions are determined by matching the solutions at the boundaries of these regions. This is in fact quite a powerful technique to estimate outgoing amplitudes in different areas of physics, such as optics and quantum mechanics. As is customary in the cosmology community, we will refer to this technique as *gluing method*. The precision of this technique depends on how smoothly the solutions of different intervals merge to each other. Depending on the intended accuracy, one can always divide the domain in more regions. Nonetheless, doing that might not necessarily provide additional intuitions or advantages compared to numerical methods.

To highlight this point, we review the gluing method for the mode equation of the standard Lorentzian dispersion relation. This example will help us understand one source of offsets when we deal with more complicated modified dispersion relations. In this vanilla model, the mode equation for a massless spectator field ϕ on the de Sitter background (with scale factor $a = -1/H\,\tau$) and minimally coupled to gravity is

$$u_k'' + \left(k^2 - \frac{2}{\tau^2}\right) u_k = 0 \ . \tag{4.2}$$

Here u represents the canonical variable defined as $u \equiv a\,\phi$. This equation is the modified Bessel equation and we can find exact solutions and the corresponding power spectrum. Assuming Bunch-Davis initial conditions, the exact modes are given by

$$u_k = \frac{1}{\sqrt{2}}\, e^{-i\,k\,\tau} \left(1 - \frac{i}{k\,\tau}\right). \tag{4.3}$$

Substituting this solution into the power spectrum,

$$P_k^\phi \equiv \frac{k^3}{2\,\pi^2} \langle\, \phi_k^2 \,\rangle = \frac{k^3}{2\,\pi^2\,a^2} \langle\, u_k^2 \,\rangle \ , \tag{4.4}$$

one obtains that at late times ($\tau \to 0$),

$$P_{\rm BD} \equiv P_k^{\phi\ (\rm exact)} = \frac{H^2}{4\pi^2} \ . \tag{4.5}$$

In the following, we will use this value as our reference point and evaluate corrections with respect to this value.

Suppose we now try to estimate the power spectrum via a gluing approach. We divide the time domain $\tau \in (-\infty, 0)$ into two regions, namely region I $= \left(-\infty, -\sqrt{2}/k\right]$ and region II $= \left[-\sqrt{2}/k, 0\right)$. We then impose continuity of the solutions and their first derivatives at the boundary point

$$\tau_b \equiv -\frac{\sqrt{2}}{k} \, . \tag{4.6}$$

In the limit $\tau \ll \tau_b$, Eq. (4.2) simplifies to a simple harmonic oscillator. The particular solution of this equation that approaches the Bunch-Davies vacuum is given by

$$u_{k\,\mathrm{I}} = \frac{1}{\sqrt{2\,k}} \exp(-i\,k\,\tau) \, . \tag{4.7}$$

On the other hand, one can neglect k^2 in Eq. (4.2) for $\tau \gg \tau_b$. Therefore, the general solution in the second region is given by

$$u_{k\,\mathrm{II}} = C_1 \tau^2 + \frac{C_2}{\tau} \, . \tag{4.8}$$

The coefficients C_1 and C_2 can be determined by assuming $u_{k\,\mathrm{I}}$ and $u_{k\,\mathrm{II}}$ remain good approximations around the boundary point τ_b, and requiring the continuity of the function and its derivative at this point,

$$u_{k\,\mathrm{I}}(\tau_b) = \qquad\qquad u_{k\,\mathrm{II}}(\tau_b) \tag{4.9}$$

$$\left.\frac{du_{k\,\mathrm{I}}(x)}{d\tau}\right|_{\tau_b} = \qquad\qquad \left.\frac{du_{k\,\mathrm{II}}(x)}{d\tau}\right|_{\tau_b} \, . \tag{4.10}$$

These conditions yield

$$C_1 = \qquad\qquad \frac{1}{12}\left(\sqrt{2} + 2\,i\right) e^{i\sqrt{2}}\, k^{3/2} \tag{4.11}$$

$$C_2 = \qquad\qquad -\frac{2 - i\,\sqrt{2}}{3\,k^{3/2}}\, e^{i\sqrt{2}} \, , \tag{4.12}$$

and the power spectrum (4.4) becomes

$$P_k^\phi \approx \frac{k^3 H^2}{2\,\pi^2}\,|C_2|^2 \approx \frac{12}{9}\frac{H^2}{4\pi^2} \approx 1.33\, P_k^{\phi\ (\mathrm{exact})} \, . \tag{4.13}$$

The discrepancy between the gluing result and the one obtained from the exact normalized modes is almost 33%, which shows the inadequacy of the gluing technique in properly estimating the amplitude of the power spectrum.

Of course, the reason for this discrepancy is that our approximate solutions in region I (4.7) and in region II (4.8) are not a good description of the actual solution in the neighbourhood of the turning point τ_b. If the regions of the validity of these solution had overlapped, then one would expect that the corresponding power spectrum be a good approximation for the exact expression. In fact, similarly to tunnelling problems in quantum mechanics, one could improve the accuracy by employing a WKB approximation in the first region and Airy functions around the turning point τ_b. We should remark that, in inflationary backgrounds unlike most tunnelling problems, the WKB approximation is not restored after crossing the turning point. To summarize, matching techniques are helpful to estimate the power spectrum, but when it comes to small corrections, one should be aware of the limitations that come with this approximation.

4.3 Corley-Jacobson dispersion relation

We now turn our attention to the simplest correction to Lorentzian dispersion relation, namely the Corley-Jacobson (CJ) dispersion relation [27] [1]. This dispersion relation assumes an additional quartic term to the physical momenta in the Ultra Violet (UV) regime,

$$\omega_{\rm ph}^2 = k_{\rm ph}^2 + \beta_0\, k_{\rm ph}^4 \ . \tag{4.14}$$

Changing to comoving momenta, $k = a\, k_{\rm ph}$ and $\omega^2(k), = a^2\, \omega_{\rm ph}^2(k/a)$ the new mode equation becomes

$$u_k'' + \left(\epsilon\, \tau^2\, k^4 + k^2 - \frac{2}{\tau^2}\right) u_k = 0 \ , \tag{4.15}$$

where we also defined the parameter $\epsilon \equiv \beta_0\, H^2$. This mode equation was extensively analyzed in Ref. [13]. It was shown there that it has exact analytical solutions and the power spectrum can again be obtained without any approximations. Imposing adiabatic vacuum initial conditions, the exact modes are given by

$$u_k^{(\rm exact)}(\tau) = \frac{\exp(-\frac{\pi}{8\,\epsilon})}{\sqrt{-2\,\epsilon\,\tau}\, k}\, {\rm WW}\left(\frac{i}{4\,\epsilon}, \frac{3}{4}, -i\,\epsilon\, k^2\, \tau^2\right) \ , \tag{4.16}$$

[1] Please also see [37] for such modified dispersion for gravitino in the context of Effective Field Theory.

with WW representing the Whittaker W function. Computing the power spectrum (4.3), one obtains

$$P_k^{\phi\ (\text{exact})} = \gamma^{(\text{exact})}\, P_{\text{BD}}\ , \tag{4.17}$$

where the modulation of the Bunch-Davis power spectrum (4.5) is given by

$$\gamma^{(\text{exact})} = \frac{\pi\, e^{-\frac{\pi}{4\,\epsilon}}}{4\,\epsilon^{3/2}\,\Gamma\left(\frac{5}{4}-\frac{i}{4\,\epsilon}\right)\Gamma\left(\frac{5}{4}+\frac{i}{4\,\epsilon}\right)}\ . \tag{4.18}$$

In order to determine the Bogolyubov coefficients, we note that Eq. (4.15) reduces to the usual vanilla one in an expanding background as $x \to 0$. Therefore, the exact solution (4.16) in this limit can be matched smoothly to an excited mode,

$$u_{k\,\text{IV}} = \frac{\sqrt{-x\,\pi}}{2}\left[\xi\, H^{(1)}_{3/2}(-x) + \rho\, H^{(2)}_{3/2}(-x)\right]\ , \tag{4.19}$$

We can then obtain the corresponding Bogolyubov coefficients ξ and ρ. Since the mode function (4.19) itself is singular at $x = 0$, instead we work with function $f(x) = x\,u(x)$ for which

$$f(0) = -i\,\frac{\xi-\rho}{\sqrt{2}} \tag{4.20}$$

$$f'(0) = 0 \tag{4.21}$$

$$f''(0) = -i\,\frac{\xi-\rho}{\sqrt{2}} = f(0) \tag{4.22}$$

$$f'''(0) = -\sqrt{2}\,(\xi+\rho)\ . \tag{4.23}$$

The Bogolyubov coefficients are then determined by evaluating the function f and its third derivative at $x = 0$. We obtain

$$\rho(\epsilon) = \frac{\sqrt{\pi}\,e^{-\frac{\pi}{8\,\epsilon}}}{4\,\epsilon^{3/2}}\left[\frac{8\,(-1)^{3/8}\,\epsilon^{9/4}}{\Gamma\left(-\frac{\epsilon+i}{4\,\epsilon}\right)} - \frac{(-i\,\epsilon)^{3/4}}{\Gamma\left(\frac{5}{4}-\frac{i}{4\,\epsilon}\right)}\right] \tag{4.24}$$

$$\xi(\epsilon) = \frac{\sqrt{\pi}\,e^{-\frac{\pi}{8\,\epsilon}}}{4\,\epsilon^{3/2}}\left[\frac{8(-1)^{3/8}\epsilon^{9/4}}{\Gamma\left(-\frac{\epsilon+i}{4\,\epsilon}\right)} + \frac{(-i\,\epsilon)^{3/4}}{\Gamma\left(\frac{5}{4}-\frac{i}{4\,\epsilon}\right)}\right]\ . \tag{4.25}$$

The number density of particles in an excited state is then given by

$$N_k(\epsilon)^{\text{exact}} = \frac{(-1)^{5/8}\,e^{-\frac{\pi}{4\epsilon}}}{32\,\pi\,\epsilon^3}\,\cosh\left(\frac{\pi}{2\,\epsilon}\right)\left[(-1)^{3/8}\,(i\,\epsilon)^{3/4}\,\Gamma\left(\frac{i-\epsilon}{4\,\epsilon}\right) - 8\,\epsilon^{9/4}\,\Gamma\left(\frac{5}{4}+\frac{i}{4\epsilon}\right)\right]\ , \tag{4.26}$$

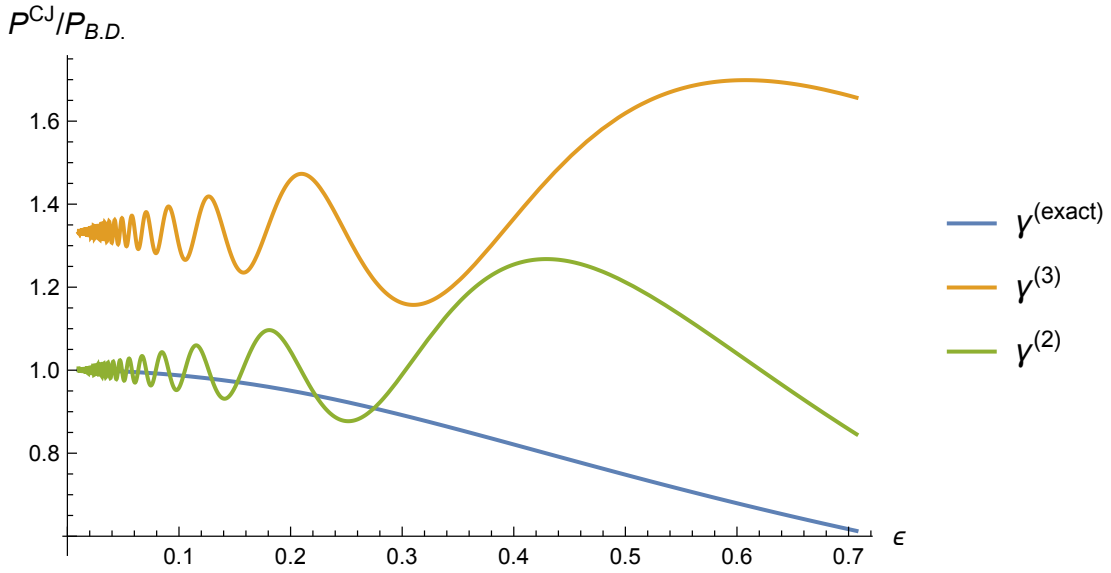

Figure 4.1: Ratio of Corley-Jacobson power spectrum to Bunch-Davies power spectrum from various methods: $\gamma^{(3)}$ is the modulation factor when using three regions for gluing solutions; $\gamma^{(2)}$ is the modulation factor when using two regions for matching solutions; and $\gamma^{(\text{exact})}$ is the exact modulation factor. Notice that, beside the superimposed oscillations, further gluing at the horizon crossing causes an offset of $1/3$ with respect to the exact result around $\epsilon = 0$. Oscillations near $\epsilon = 0$ are an artefact introduced by the gluing technique and are absent in the exact result.

which goes like $25\,\epsilon^4/64$ for small ϵ.

Now that we have the exact answer, we can again check the precision of the gluing technique. As noted previously in Ref. [13], assuming $\epsilon \ll 1/\sqrt{2}$, one can decompose the time domain into three regions:

$$k\,\tau \leq -\epsilon^{-1} \qquad \text{region I} \tag{4.27}$$

$$-\epsilon^{-1} \leq k\,\tau \leq -\sqrt{2} \qquad \text{region II} \tag{4.28}$$

$$k\,\tau \geq -\sqrt{2} \qquad \text{region III}\ . \tag{4.29}$$

The solution in region I that satisfies the wronskian condition,

$$u(\tau)\,u'^{*}(\tau) - u^{*}(\tau)\,u'(\tau) = i\ , \tag{4.30}$$

and the adiabatic vacuum initial conditions, turns out to be

$$u_{k\,\mathrm{I}} = \frac{D_{-\frac{1}{2}}\left((-1)^{3/4}\,\sqrt{2\,\epsilon}\,x\right)}{(2\,\epsilon)^{1/4}\,\sqrt{k}}\ . \tag{4.31}$$

Here, $D_\nu(x)$ is the parabolic cylinder function of order ν, and we defined the dimensionless parameter $x \equiv k\,\tau$. Next, this solution is glued to the general solutions in region II,

$$u_{k\,\mathrm{II}} = A_2\,\exp(i\,x) + B_2\,\exp(-i\,x)\ , \tag{4.32}$$

and the coefficients are determined by requiring continuity at $x_1 = -1/\epsilon$. This yields

$$A_2 = -\frac{(1+i)\,e^{i/\epsilon}\left[\sqrt{\epsilon}\,D_{\frac{1}{2}}\left(\frac{1-i}{\sqrt{\epsilon}}\right) - (1-i)\,D_{-\frac{1}{2}}\left(\frac{1-i}{\sqrt{\epsilon}}\right)\right]}{(32\,\epsilon)^{1/4}\,\sqrt{k}} \tag{4.33}$$

$$B_2 = \frac{(1+i)\,e^{-i/\epsilon}\,\sqrt[4]{\epsilon}\,D_{\frac{1}{2}}\left(\frac{1-i}{\sqrt{\epsilon}}\right)}{2\,\sqrt[4]{2}\,\sqrt{k}}\ . \tag{4.34}$$

Likewise, matching these solutions to the general solutions in region III,

$$u_{k\,\mathrm{III}} = \frac{A_3}{x} + B_3\,x^2\ , \tag{4.35}$$

leads to

$$A_3 = \frac{e^{-\frac{i\left(\sqrt{2}\,\epsilon+1\right)}{\epsilon}}}{3\,\sqrt[4]{8\,\epsilon}\,\sqrt{k}}\,\left\{(1+i)\,\sqrt{\epsilon}\left[\left(2+i\,\sqrt{2}\right)e^{2\,i/\epsilon} + i\,\left(\sqrt{2}+2\,i\right)e^{2\,i\sqrt{2}}\right]D_{\frac{1}{2}}\left(\frac{1-i}{\sqrt{\epsilon}}\right)\right.$$
$$\left. -\left(4+2\,i\,\sqrt{2}\right)e^{2\,i/\epsilon}\,D_{-\frac{1}{2}}\left(\frac{1-i}{\sqrt{\epsilon}}\right)\right\} \tag{4.36}$$

$$B_3 = \frac{(1+i)\,e^{-\frac{i\left(\sqrt{2}\,\epsilon+1\right)}{\epsilon}}}{12\,\sqrt[4]{8\,\epsilon}\,\sqrt{k}}\,\left\{\sqrt{\epsilon}\left[\left(\sqrt{2}+2\,i\right)e^{2\,i\,\sqrt{2}} - \left(\sqrt{2}-2\,i\right)e^{2\,i/\epsilon}\right]D_{\frac{1}{2}}\left(\frac{1-i}{\sqrt{\epsilon}}\right)\right.$$
$$\left. +(1-i)\left(\sqrt{2}-2\,i\right)e^{2\,i/\epsilon}D_{-\frac{1}{2}}\left(\frac{1-i}{\sqrt{\epsilon}}\right)\right\}\ . \tag{4.37}$$

The power spectrum is finally obtained to be

$$P^{(3)}_{\mathrm{CJ}} \equiv \gamma^{(3)}\,P_{\mathrm{BD}} = 2\,|A_3|^2\,P_{\mathrm{BD}}\ . \tag{4.38}$$

In fig. 4.1, we plotted the factor $\gamma^{(3)}$ as a function of ϵ. One can see that the factor $\gamma^{(3)}$ oscillates around 4/3 for small values of ϵ, with an amplitude roughly proportional to ϵ. This oscillatory behaviour continues for larger values of ϵ, up to the point of validity of the above computation. Note that when we are matching two oscillatory solutions at high frequencies we expect the error to oscialite as well. As we see the exact result does not show any oscillations, but only a suppression proportional to $-\epsilon^2$ close to $\epsilon \approx 0$. The large offset of 1/3 from the exact result is reminiscent of the discrepancy observed in the previous section from gluing the modes at the horizon crossing point, $x = -\sqrt{2}$. In fact, the offset can be removed if the regions II and III are combined. The improved solutions in this unified region, (4.19), can then be glued to the solution in region I. As we see in fig. 4.1, the modulation factor $\gamma^{(2)}$ obtained using just two region does not show any offset from the exact result anymore. This result still displays an oscillatory feature for small values of the distortion parameter ϵ, which is again due to the inadequacy of this technique in the UV.

The number of particles obtained from the gluing technique with two-regions is

$$\begin{aligned} N_k^{(2)}(\epsilon) = & \frac{\pi}{4\sqrt{2}\,\epsilon^{3/2}} \left\{ D_{-\frac{1}{2}}\left(\frac{1-i}{\sqrt{\epsilon}}\right) \left[H^{(1)}_{\frac{1}{2}}(\epsilon^{-1}) - (\epsilon - i)\, H^{(1)}_{\frac{3}{2}}(\epsilon^{-1})\right] \right. \\ & \left. + (1-i)\sqrt{\epsilon}\, D_{\frac{1}{2}}\left(\frac{1-i}{\sqrt{\epsilon}}\right) H^{(1)}_{\frac{3}{2}}(\epsilon^{-1}) \right\} \times \left\{ (1+i)\sqrt{\epsilon}\, D_{\frac{1}{2}}\left(\frac{1+i}{\sqrt{\epsilon}}\right) H^{(2)}_{\frac{3}{2}}(\epsilon^{-1}) \right. \\ & \left. + D_{-\frac{1}{2}}\left(\frac{1+i}{\sqrt{\epsilon}}\right) \left[H^{(2)}_{\frac{1}{2}}(\epsilon^{-1}) - (\epsilon + i)\, H^{(2)}_{\frac{3}{2}}(\epsilon^{-1})\right] \right\} , \end{aligned} \tag{4.39}$$

which behaves like $\epsilon^2/16$ for small ϵ, as opposed to $25\,\epsilon^4/64$ for the exact solution. In fig. 4.2, we have plotted both the number of particles obtained by the gluing method and the one from the exact mode functions. It displays it clearly that the number of particles for exact solution goes to zero faster than what the gluing method predicts for small ϵ, .

4.4 Sixth order polynomial dispersion relation

We are now going to take one step further and investigate mode equations of the form (4.1), where the dispersion relation is governed by $\omega^2 \propto k^6$ in the infinite past. In particular we consider the cases that perturbation modes start from adiabatic vacuum, then go through a non-adiabatic phase where group velocity becomes negative and finally re-emerge as super-excited states when $\omega^2 \simeq k^2$. For convenience we have set the sound speed in (4.1)

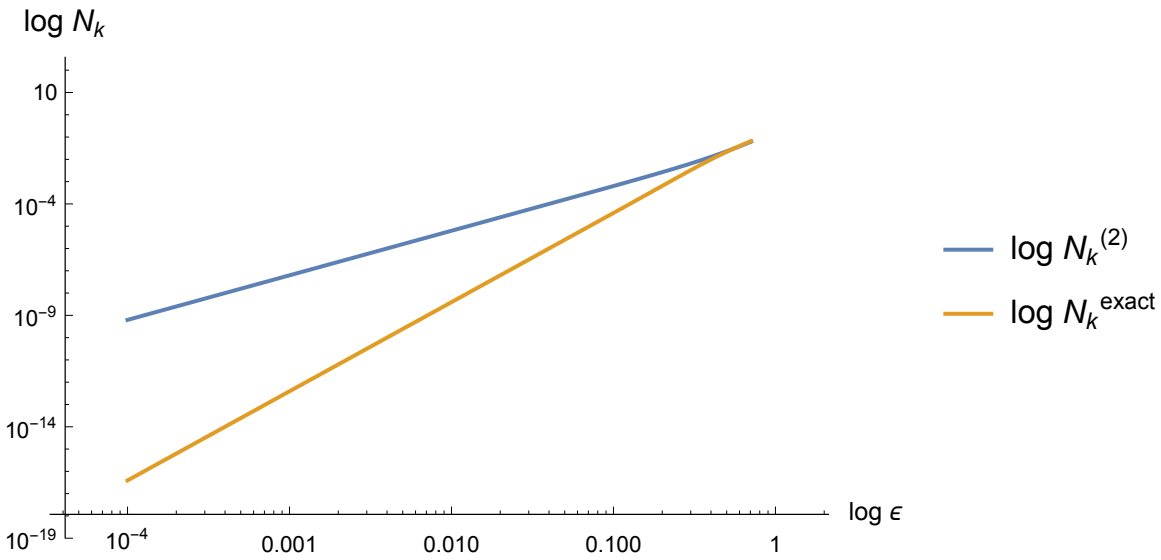

Figure 4.2: Number of particles in the corresponding excited states obtained via gluing is compared to the exact one as function of ϵ . The exact number of particles goes to zero faster by an extra factor of ϵ^2.

to unity [2]. Implementing this dispersion for the the canonicalized variable u, mode equation takes the following form

$$u_k'' + \left(\beta_0\, x^4 - \alpha_0\, x^2 + 1 - \frac{2}{x^2}\right) u_k = 0 \ , \tag{4.40}$$

where $x \equiv k\tau$ as before, $\beta_0 \equiv \bar{\beta} H^4$ and $\alpha_0 \equiv \bar{\alpha} H^2$. As we will discuss in section **??**, these dispersion relations can be realized, in the effective field theory of inflation [25], from terms like $\nabla_\mu \delta K^{\nu\gamma}\, \nabla^\mu \delta K_{\nu\gamma}$, $(\nabla_\mu \delta K^\nu{}_\nu)^2$, $\nabla^\mu \delta K_{\nu\mu} \nabla^\nu \delta K^\sigma_\sigma$ and $\nabla_\mu \delta K^\mu{}_\nu\, \nabla_\gamma \delta K^{\gamma\nu}$. A similar dispersion relation has also come up in the study of trans-Planckian signatures in inflation [43, 36]. We can constraint the dispersion relation (4.1) to be nonnegative (non-tachyonic) at all sub Hubble scales by setting [36],

$$z \equiv \frac{\beta_0}{\alpha_0^2} \geq \frac{1}{4} \, . \tag{4.41}$$

[2] If $c_s \neq 1$, one can still make it to one in mode equation for the canonical variable u, by changing the conformal time $d\tau \to c_s d\tau$. When evaluating the power spectrum for field ϕ or curvature perturbations that factor will reemerge.

To be on the conservative side, we also assume that the modes get lighter than the Hubble scale only once during inflation, which corresponds to the time of horizon-crossing, i.e $\omega^2 = 2H^2$ has only one solution which is around $k \sim 1/aH$. This is different from the study of Ref. [36], where it was assumed that there are three turning points corresponding to three solutions of the equation $\omega^2 - 2\,H^2 = 0$. For

$$z > \frac{1}{3}, \tag{4.42}$$

this equation automatically has only one solution. For values of α_0 and β_0 such that

$$\frac{1}{4} \leq z \leq \frac{1}{3}\,, \tag{4.43}$$

having only one solution imposes one of the following conditions

$$\begin{aligned} \alpha_0 \leq & \quad \frac{9z - 2 - 2(1-3z)^{3/2}}{54z^2} \\ \text{or} \quad \alpha_0 \geq & \quad \frac{9z - 2 + 2(1-3z)^{3/2}}{54z^2}\,. \end{aligned} \tag{4.44}$$

Again, we will first try to estimate the particle number density using the gluing approach. We decompose the domain of $x \equiv k\tau \in (-\infty, 0]$ into the intervals

$$-\infty < x \lesssim x_1(\alpha_0, \beta_0) \qquad \text{region I} \tag{4.45}$$

$$x_1(\alpha_0, \beta_0) < x < 0 \qquad \text{region II} \tag{4.46}$$

where $x_1(\alpha_0, \beta_0)$ is the transition point below which the higher order corrections to the dispersion relation can be neglected and the mode equation becomes the stabdard Lorentzian dispersion relation. In general $x = x_1(\alpha_0, \beta_0)$ can be determined by solving the equation

$$\alpha_0 x^4 - \beta_0 x^2 = 1 - \frac{2}{x^2}\ , \tag{4.47}$$

and is a complicated function of α_0 and β_0, but we note that for the cases of our interest $\beta_0 \sim \alpha_0^2$, and one has

$$x_1(\alpha_0, \beta_0) \approx -\frac{2}{\sqrt{\alpha_0}}\,. \tag{4.48}$$

Interestingly, Maple can find a compact solution in terms of Heun T functions to the mode equation if the term $2/x^2$ was dropped. Therefore this solution is applicable to region I.

After normalizing it according to the Wronskian condition (4.30), and imposing adiabatic vacuum initial condition, we obtain

$$u_{k\,\mathrm{I}}(x) = \frac{\beta_0^{1/4}}{k^{1/2}\,\alpha_0^{1/2}}\mathrm{HeunT}(\mathscr{A}, 0, \mathscr{B}, -\mathscr{C}\ x)\ \exp(-y)\ , \tag{4.49}$$

where

$$\begin{aligned}
\mathscr{A} &= \frac{1}{32}\,\frac{{\alpha_0}^2 18^{1/3}\left(i\sqrt{3}+1\right)^2}{{\beta_0}^{4/3}} \\
\mathscr{B} &= -\frac{1}{4}\,\frac{\alpha_0\,\sqrt[3]{12}\left(i\sqrt{3}+1\right)}{{\beta_0}^{2/3}} \\
\mathscr{C} &= -\frac{1}{3}\,3^{2/3}\sqrt[3]{2}\sqrt[6]{\beta_0}\sqrt[6]{-1}\ ,
\end{aligned} \tag{4.50}$$

and

$$y = \frac{1}{12}\,\frac{x\left(-4\,i\beta_0\,x^2 + 3\,\sqrt{3}\,(-1)^{2/3}\,\alpha_0 + 3\,\sqrt[6]{-1}\alpha_0\right)}{\sqrt{\beta_0}}\ . \tag{4.51}$$

This solution has to be matched to the general solution in region II, which is nothing other than a linear combination of Hankel functions (4.19),

$$u_{k\,\mathrm{II}} = \frac{\sqrt{-x\pi}}{2\sqrt{k}}\left[\xi\,H^{(1)}_{3/2}(-x) + \rho\,H^{(2)}_{3/2}(-x)\right]\ . \tag{4.52}$$

The solutions should be glued following the same prescription as (4.9) and (4.10) at the point $x_g = x_1(\alpha_0, \beta_0)$.

For $\alpha_0 = 0.2$ and

$$\frac{\alpha_0^2}{4} \leq \beta_0 \leq \frac{\alpha_0^2}{3} \tag{4.53}$$

Eqs. (4.44) is satisfied. For larger ratios of β_0/α_0^2, although one can solve for the Bogolyubov coefficients implicitly in terms of Heun T and Heun T Prime functions, Maple software cannot evaluate the values of these parameters numerically. Apparently Maple employs a series expansion for the Heun T Prime function which does not converge for such range of parameters. For $\alpha_0 = 0.2$, the enhancement factor for power spectrum is in the following range

$$183.35 \leq \gamma \leq 454.89, \tag{4.54}$$

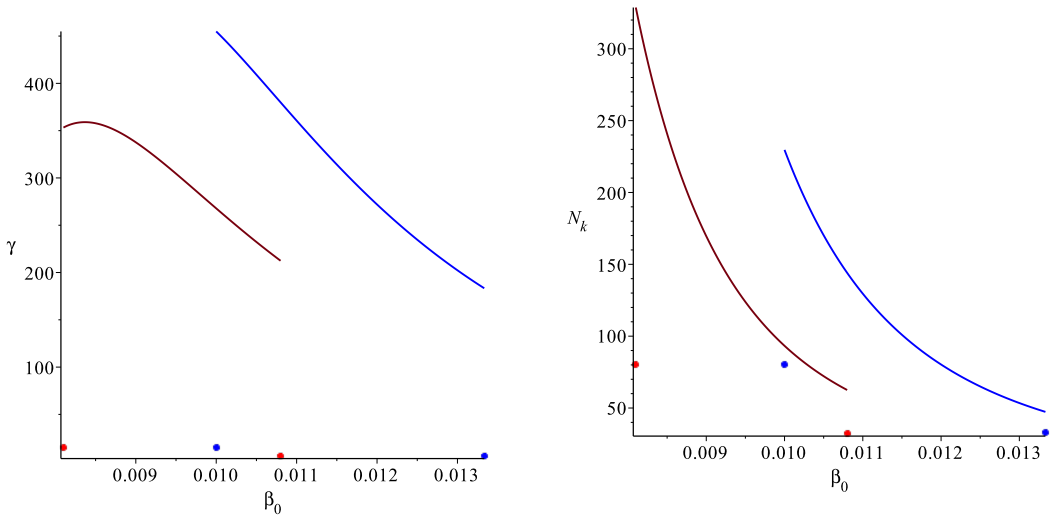

Figure 4.3: Power spectrum enhancement (left panel) and occupation number (right panel) obtained with gluing method (red and blue curves) compared to full numerical result (dots). For few values of α_0 and β_0, we have computed the correction to the power spectrum and the number of particles in the corresponding excited state numerically. The difference between these dots and the corresponding point on the curves shows that the gluing method could have a large error in estimating these parameters. The blue and red curves (dots), correspond to $\alpha_0 = 0.2$ and $\alpha_0 = 0.18$, respectively.

which is quite large. The range for number of particles in the excited state, N_k, is

$$47.31 \leq N_k \leq 229.63 \tag{4.55}$$

In Fig. 4.3, we have plotted γ and N_k for $\alpha_0 = 0.2$ and $\alpha_0 = 0.18$, in the range $\frac{1}{4} \leq z \leq \frac{1}{3}$. Such values of α_0 satisfy the constraints (4.44) and thus there is only one turning point corresponding to the horizon crossing. As we discussed in the last section, the gluing technique can become unreliable in obtaining the enhancement parameter and the number of particle. Thus, one may wonder to what extent the above results can be trusted. The following derivation shows that in fact, compared to the numerical result, gluing method significantly overestimates the occupation number of excited states and the enhancement factor.

Although one cannot find the exact power spectrum parametrically as a function of α_0 and β_0, we can still compute the power spectrum numerically for fixed values of these

parameters. Starting from the normalized positive frequency WKB mode in the infinite past,

$$u_k(x \to -\infty) \simeq \frac{1}{2}\left(-\frac{\pi}{3}x\right) H^{(1)}_{\frac{1}{6}}\left(-\frac{\sqrt{\beta_0}}{3}\,x^3\right) \ , \tag{4.56}$$

the solution is then evolved numerically. Table 5.1, lists the values of the enhancement factor and other variables evaluated numerically, for given pairs of (α_0, β_0). The largest enhancement for the power spectrum occurs when $\alpha_0 \simeq 0.2$ and $\beta_0 \simeq \alpha_0^2/4$ and, for illustration purposes, we focus on these particular values of parameters. The enhancement factor over the Bunch-Davies result for the power spectrum is about $\gamma = 14.738$. This is much smaller than the enhancement factor, $\gamma = 454.89$, obtained through gluing. Contrary to the adiabatic case, the gluing technique fails by a huge amount with respect to the numerical result.

Although Mathematica does not recognise any compact explicit solution for the mode equation (4.40) inside the horizon, it can come up with implicit solutions for the complete mode equation, which formally read as

$$u_k(x) = c_1\, u_k^{(1)}(x) + c_2\, u_k^{(2)}(x) \ , \tag{4.57}$$

where c_1 and c_2 satisfy

$$c_1\, \bar{c_2} - c_2\, \bar{c_1} = i \ . \tag{4.58}$$

The solutions $u_k^{(i)}$, with $i = 1, 2$, are normalized so that for one of them $u_k^{(i)}(1) = 1$ and $u_k^{(i)'}(1) = 0$ and for the other one it is the other way around[3]. The most general solutions to the Wronskian condition with real c_1 is

$$c_1 = \frac{1}{\sqrt{2}\, s} \tag{4.59}$$

$$c_2 = -i\frac{s}{\sqrt{2}} \ , \tag{4.60}$$

where $s \in \mathbb{R}$. We determine the parameter s, by requiring that the power spectrum obtained from the modes (4.57) matches the one obtained by numerically evolving the initial condition (4.56). There are usually four different solutions, two by two negative of each other. For all these values of s, one can compute the corresponding implicit mode function and we choose the one which leads to almost the same value of the mode

[3]It turns out that these implicit solutions are much easier to evaluate if their argument is real and positive. Noting that the differential equation is even under $x \to -x$, we will work in the domain $(0, \infty)$, instead of $(-\infty, 0)$.

function obtained by integrating numerically the mode equation. In principle, one can then follow the steps taken in the previous section to determine the number of particles in the corresponding state. However, while the amplitude of fluctuations, which is proportional to $f(x) \equiv x\, u_k(x)$, approaches a constant value outside the horizon, the way Mathematica numerically solves the equation, the error accumulates in higher derivative terms such as f''', and make them diverges as $x \to 0$. What we do instead is the following, we expect the general solution of (4.40) to merge quite well to Henkel functions even before Hubble crossing. Therefore, we glue the mode function (4.57) to a linear combination of Hankel functions at an *arbitrary* point x_g. We next demand the corresponding Bogolyubov coefficients $\xi(x_g)$ and $\rho(x_g)$ yield the numerically computed value for the power spectrum. We then test our solution to make sure our assumption for gluing at x_g is justified. For $\alpha_0 = 0.2$ and $\beta_0 = \alpha_0^2/4$, we have plotted both the real and imaginary parts of the implicit numerical solution and the excited one obtained though matching the linear combination of Hankel functions (see fig. 4.4). In this case $x_g = 1.2145$, and as the figure displays these functions merge very well at that point. The values of the Bogolyubov coefficients estimated at this point are

$$\xi(x_g) = 1.95519 - 8.80935\, i \qquad \rho(x_g) = -1.88359 - 8.7681\, i \ , \tag{4.61}$$

which suggests that the particle number density in the corresponding excited state is $N_k = 80.4275$. This number is quite large and suitable to serve as a highly excited state above the Bunch-Davies vacuum. In the language of [15], this corresponds to $\chi_S \simeq 2.19$, which is enough to serve our interests.

In table 5.1, we also list the corresponding values of the Bogoliubiov coefficients that yields the correct enhancement factor to the power spectrum.

We note in passing that it is also possible to produce the so called "calm excited states". [17], with this type of dispersion relations. One can cook up values for α_0 and β_0 that lead to excited states but do not modify the power spectrum at all. For example, with

$$\alpha_0 = \qquad 0.0101982725 \ , \tag{4.62}$$

$$\beta_0 = \qquad \frac{\alpha_0^2}{3} \ , \tag{4.63}$$

one obtains an excited state with Bogolyubov coefficients

$$\rho = \qquad -0.320196 - 2.16841\, i \ , \tag{4.64}$$

$$\xi = \qquad 0.669079 - 2.31449\, i \ , \tag{4.65}$$

and particle number density $N_k \simeq 4.80453$. Nonetheless, the impact of such an excited state on the two-point function is negligible. Therefore, one cannot say conclusively if the mode has originated from an excited state just by examining the power spectrum.

α_0	β_0	γ	ρ	ξ	N_k
0.1	$\alpha_0^2/3$	2.62652	$-0.727078 - 3.65736\ i$	$0.890536 - 3.75658\ i$	13.9049
0.18	$\alpha_0^2/4$	14.7378	$1.88601 + 8.77648\ i$	$-1.95745 + 8.81771\ i$	80.5836
0.18	$\alpha_0^2/3$	5.95909	$-1.16428 - 5.55538\ i$	$1.27598 - 5.62047\ i$	32.2178
0.19	$\alpha_0^2/4$	14.7739	$-1.88609 - 8.77973\ i$	$1.95736 - 8.82098\ i$	80.641
0.19	$\alpha_0^2/3$	5.95909	$-1.16407 - 5.55488\ i$	$1.27619 - 5.61989\ i$	32.2118
0.2	$\alpha_0^2/4$	14.738	$-1.88359 - 8.7681\ i$	$-1.95519 + 8.80935\ i$	80.4275
0.2	$\alpha_0^2/3$	6.06496	$-1.17517 - 5.60415\ i$	$1.2867 - 5.6685\ i$	32.7875
0.3	$\alpha_0^2/4$	12.838	$-3.66837 + 1.44445\ i$	$1.83104 - 8.21655\ i$	69.8644
0.3	$\alpha_0^2/3$	6.06576	$-1.17328 - 5.59953\ i$	$1.28877 - 5.66307\ i$	32.7313
0.4	$\alpha_0^2/4$	10.6292	$-1.58475 - 7.42534\ i$	$1.67516 - 7.47268\ i$	57.647
0.4	$\alpha_0^2/3$	5.44107	$-1.10289 - 5.29483\ i$	$-4.44333 + 1.44564\ i$	29.2516
0.5	$\alpha_0^2/4$	8.87117	$-1.43795 - 6.77284\ i$	$1.54006 - 6.82402\ i$	47.939
0.5	$\alpha_0^2/3$	4.79253	$1.16308 - 5.03005\ i$	$-1.02498 - 4.9602\ i$	25.6542

Table 4.1: Modulation factor γ, Bogolyubov coefficients ξ and ρ, and particle number density N_k for the sixth order dispersion relation.

4.5 Effective Field Theory

Effective field theory is a technique in which the relevant low-energy degrees of freedom are isolated yet the effects of high-energy degrees of freedom are systemically included[53]. This sounds obvious in most fields of physics. Quantum effects or multipole expansions are both ignored in classical scales, or at a large distance scale. We do not need to worry about physics of small scale quantum mechanics when we want to study the orbital motions of planets.

Now, taking advantage of this scale separation in quantum field theories gives us effective field theories. The basic principle of effective field theories is the same idea as scale separation in other fields of physics. The high energy or low distance scale effects are suppressed by powers of the ratio of scales [53]. Effective field theories are everywhere, but in this section we will focus on the effective field theory of inflation.

4.5.1 Basic Principles

The first step in building effective field theories is to identify which degrees of freedom is relevant for the purpose of interest. In particle physics, light particles ϕ_L are included

in the theory, but the heavy particles ϕ_H are not [19]. However we do not always have light or heavy particles, so we characterize heavy and light degrees of freedom based on whether the particles can be generated on shell within the energies relevant to the problem of interest.

Effective Actions and Lagrangian

Since the heavy degrees of freedom are integrated out by a path integral, so we have an effective action given by

$$e^{iS_{eff}(\phi_L)} \equiv \int \mathcal{D}\phi_H e^{iS(\phi_L,\phi_H)}. \tag{4.66}$$

The effective Lagrangian contains a finite number of renormalizable terms of dimension four or less and a infinite number of non-renormalizable terms of dimensions bigger than four [19],

$$\mathcal{L}_{eff}(\phi_L) = \mathcal{L}_{\Delta<4} + \sum_i c_i \frac{\mathcal{O}_i(\phi_L)}{\Lambda^{\Delta_i-4}}, \tag{4.67}$$

where Δ_i denote the deminsions of the operators $\mathcal{O}_i$, and $\mathcal{O}_i$ are the operators local in space-time for the energy scales less than the mass of the heavy particles [19]. Although the sum of the operators $\mathcal{O}_i$ is an infinite sum, only a few terms are relevant. Not all the terms needs to be kept because the higher the diemsnion of an operator, the smaller the contribution to low-energy observables [19]

4.5.2 Effective Field Theory in Inflation

In the onctext of inflation, the relevant energy scale is $E \sim H$. Then the effective field theory consists at least one light scalar field, the inflaton, denoted as ϕ in this section. Also we will have all the operators consistent with the symmetries of ϕ,

$$\frac{\mathcal{O}_\delta}{\Lambda^{\delta-4}}, \tag{4.68}$$

where δ is the mass dimension of the corresponding operator [19].

Sensitivity

In effective field theories, the larger the cut off Λ is, the more suppressed the effects of $\mathcal{O}_\delta$ is. However, since the known physics is up to the Planck-scale, the largest cutoff we

can make is the Planck-scale. Also, as mentioned, operators of very high dimsions become irrelevant because they decouple in the low-energy limit. Thus, in most of particle physics, very high dimensional operators and Planck-scale processes become irrelevant. However, in inflation, the flatness of potential in Planck units makes the theory sensitive to the case of $\delta \leq 6$ Planck-suppressed operators [19],

$$\frac{\mathcal{O}_6}{M_p^2}. \tag{4.69}$$

4.6 Effective Field theory of Inflation

In the previous section, the basic idea and principles of inflation were introduced. In this section, using the same principles, we set up the effective field theory of inflation. To do so, we look at inflation as the inflation as the theory of a Goldstone boson [49] [25].

4.6.1 Goldstone Boson

Consider a simple theory of a $U(1)$ global symmetry given by $\phi \to e^{i\alpha}\phi$ that is spontaneously broken by the mexican hat like potential $\phi \to < \phi >$. In this theory, we have Goldstone boson π that gives us the symmetry $\pi \to \pi + \alpha$ [49]. The Lagrangian of a complex scalar field, ϕ, given by

$$\mathcal{L} = \partial_\mu \phi^* \partial^\mu \phi - m^2 \phi^* \phi + \lambda \phi^{*2} \phi^2, \tag{4.70}$$

gives us

$$\phi = \frac{m}{\lambda^{1/2}} e^{i\pi}, \tag{4.71}$$

where m is the mass. The Lagrangian of π resembles massless scalar field with a shift symmetry

$$\mathcal{L}_\pi = (\partial\pi)^2 + \frac{1}{(\frac{m}{\lambda^{1/2}})^4}(\partial\pi)^4 + ... \tag{4.72}$$

with higher derivatives suppressed by powers of the energy scale $m/\lambda^{1/2}$.

The inflation means that there existed a period of accelerated expansion of our quasi de Sitter universe. Because it had to end, this requires spontaneous time-translation breaking [25].

Now, suppose a physical clock which allows us to measure time and forces inflation to end. We can always use coordinate transformation to go to the frame where this clock is set to zero. This can be done by time translating to coordinates where the fluctuations of the clock are set to zero. For example, suppose that we have ϕ as a fundamental scalar field with $\delta\phi \neq 0$. Then we can translate time $t \to \tilde{t} + \delta t$ such that

$$\tilde{\delta\phi} = \delta\phi - \dot{\phi}_0 \delta t = 0. \tag{4.73}$$

Now we write the action with all the relevant degree of freedom, which is the metric fluctuations. We expand in fluctuations and write down all the operators corresponding to relevant symmetries of the theory [49]. Also note that we can change spatial coordinates within different spatial hypersurface in a different way meaning that the residual gauge symmetry becomes time-dependent spatial diffeomorphisms

$$x^i \to \tilde{x}^i = x^i + \xi^i(t, \vec{x}). \tag{4.74}$$

We can then expand the action in perturbations to the order that we are interested.

4.6.2 Action in Unitary Gauge

Now to write down the most general action in this gauge, we write down all the operators that are functions of the metric $g_{\mu\nu}$ and are invariant under time-dependent spatial diffeomorphisms. Since these time-dependent spatial diffeomorphisms are unbroken, we can consider inflation as "the theory of space-time diffeomorphisms spontaneity broken to time-dependent spatial diffeomorphisms [49]." The most general action then can be written as

$$S = \int d^4x\sqrt{-g}\left\{M_p^2\left[\frac{1}{2}R + \dot{H}g^{00} - \left(3H^2 + \dot{H}\right)\right] + L_n\right\}, \tag{4.75}$$

where

$$L_n = \sum_{m\geq 2}^{n} F^{(m)}(\delta g^{00}, \delta K_{\mu\nu}, \delta R_{\mu\nu\rho\sigma}; \nabla_\mu; t), \tag{4.76}$$

and $F^{(m)}$ denotes functions of order m in perturbations. $K_{\mu\nu}$ is the extrinsic curvature of the sliced hypersurface, and $R_{\mu\nu\rho\sigma}$ is the Riemann tensor.

4.6.3 Relaxing Gauge Conditions

Once we have the most general action in the unitary gauge, we can relax the gauge conditions by reintroducing time diffeomorphism invariance again. We can do this by promoting

$\xi^0(x^\mu)$ to Goldstone boson $-\pi(x^\mu)$ and setting $\pi \to \pi(x^\mu) - \xi^0(x^\mu)$ under the time diffeomorphisms [11]. Introducing the Goldstone boson, the perturbation of the scalar field ϕ is no longer set to zero. In fact, we have $\delta\phi = -\dot{\phi}_0\xi^0 \to \pi = \delta\phi/\dot{\phi}_0$.

Advantage of this approach is that as long as we are in the slow roll regime, we can ignore the metric perturbation. The reason is that when the time dependence of the coefficients in the unitary gauge is much less than the Hubble scale, then the decoupling limit is larger than the Hubble scale. Thus when we calculate the power spectrum, we can neglect the metric perturbations.

4.6.4 k^6 Modification to the Dispersion Relation

Consider the case where we expand to the zeroth order. This is equivalent to setting $L_n = 0$ and we get an action

$$S_\pi = -M_p^2 \int dx\sqrt{-g}\dot{H}\left(\dot{\pi}^2 - \frac{(\partial\pi)^2}{a^2}\right). \tag{4.77}$$

We can use gauge transformation to show that the field π is related to the conserved quantity ζ by

$$\zeta = -H\pi. \tag{4.78}$$

Now we are interested in the terms that gives us k^6 modification to the dispersion relation. Then only keeping the terms that contribute to the quadratic action of π and at most sixth order of gradient operators, L_n becomes

$$\begin{aligned} L_n \;=\; & \frac{M_2^4}{2!}(g^{00}+1)^2 - \frac{\bar{M}_2^2}{2}(\delta K^\mu{}_\mu)^2 - \frac{\bar{M}_3^2}{2}\delta K^\mu{}_\nu\,\delta K^\nu{}_\mu \\ & -\frac{\delta_1}{2}(\nabla_\mu\delta K^{\nu\gamma})(\nabla^\mu\delta K_{\nu\gamma}) - \frac{\delta_2}{2}(\nabla_\mu\delta K^\nu{}_\nu)^2 - \frac{\delta_3}{2}(\nabla_\mu\delta K^\mu{}_\nu)(\nabla_\gamma\delta K^{\gamma\nu}) \\ & -\frac{\delta_4}{2}\nabla^\mu\delta K_{\nu\mu}\nabla^\nu\delta K^\sigma_\sigma\ . \end{aligned} \tag{4.79}$$

The coefficients M_i and δ_i are time dependent free coefficients. The first line of eq. 4.79 gives us the quartic modification o the dispersion relation,

$$u'' + (\gamma_0 k^2 + a_0 k^4\tau^2 - \frac{2}{\tau^2})u = 0, \tag{4.80}$$

where γ_0 and α_0 are functions of M_i and δ_i. The second line and the third line, gives us, to the second order of π,

$$\begin{aligned}\mathcal{L}_n^{(2nd)} &= -\frac{1}{2}\delta_1\left(\frac{k^6\pi^2}{a^6}-\frac{13H^2k^4\pi^2}{a^4}+\frac{k^4\dot{\pi}^2}{a^4}+\frac{24H^4k^2\pi^2}{a^2}+\frac{2H^2k^2\dot{\pi}^2}{a^2}-6H^4\dot{\pi}^2-3H^2\ddot{\pi}^2\right)\\ &\quad -\frac{1}{2}\delta_2\left(\frac{k^6\pi^2}{a^6}+\frac{H^2k^4\pi^2}{a^4}-\frac{k^4\dot{\pi}^2}{a^4}+\frac{6H^4k^2\pi^2}{a^2}-9H^2\ddot{\pi}^2\right)\\ &\quad -\frac{1}{2}\delta_3\left(\frac{k^6\pi^2}{a^6}-\frac{10H^2k^4\pi^2}{a^4}+\frac{15H^4k^2\pi^2}{a^2}-9H^4\dot{\pi}^2\right)\\ &\quad -\frac{1}{2}\delta_4\left(\frac{k^6\pi^2}{a^6}-\frac{13H^2k^4\pi^2}{2a^4}+\frac{21H^4k^2\pi^2}{2a^2}-\frac{9H^2k^2\dot{\pi}^2}{a^2}-\frac{9}{2}H^4\dot{\pi}^2\right).\end{aligned} \tag{4.81}$$

Now the k^n, $n \geq 4$ terms do appear, but not all of them stays. For example δ_1 and δ_2 terms also produce higher time derivatives of π and this usually lead to the ghost instabilities [11]. Furthermore terms $k^2\dot{\pi}^2$ and $k^4\dot{\pi}^2$ brings the correction to the modified dispersion relation back to k^4 or k^2. Thus we set $\delta_1 - \delta_2 = \delta_4 = 0$. The only remaining term then becomes the δ_3 term.

This modification to the Lagrangian gives us the modification to the dispersion relation

$$u'' + (\gamma_0 k^2 + \alpha_0 k^4\tau^2 + \beta_0 k^6\tau^4 - \frac{2}{\tau^2})u = 0. \tag{4.82}$$

Even though such dispersion relations are in principle easy to produce within the effective field theory of inflation, it has been argued [25] that invoking dispersion relations $\omega^2 \propto k^{2n}$ with $n \geq 3$ undermines the concept of effective field theory itself. This is because for $n \geq 3$ the interaction terms scale with negative power of energy and therefore become strongly coupled at low energies. That comes from the fact that the scaling dimension of π will not be the same as the one for the Lorentzian dispersion relation. This implies that in the high momenta regime where we are invoking $\omega^2 \propto k^6$, theory has an IR cut off, below which it becomes strongly coupled. However, note that as universe expands the quartic and Lorentzian corrections to dispersion relation become more important and eventually take over. Given the different parameters that can contribute to kinetic terms, we think it is plausible to tune the IR cut off for that regime to be below the scale where dispersion relation transitions to $\omega^2 \propto k^2 - \bar{\alpha}k^4$. One may argue that this makes the theory highly fine tuned at UV. That may very well be the case, but given that we don't know what the UV complete theory is, it is hard to say what is natural and what terms are protected under the fundamental symmetries. For example Horava's proposal for a UV completion of gravity

[35] naturally predicts dispersion relation of the form $\omega \propto k^3$ for graviton, based on Lifshitz symmetry. In the end, we also expect that the overall bounds on the non-gaussianity be satisfied when speed of sound is close to one [15]. The non-gaussianity parameter, $f_{\rm NL}$, remains finite for super-excited states, since it is defined as bispectrum divided by the power spectrum squared. Even though three point functions for such super-excited states may get enhanced [52], as we showed here the power spectrum is enhanced too, so the net effect on $f_{\rm NL}$ may still remain small.

4.7 Conclusion

We constructed super-excited initial conditions around the new physics hypersurface, with the help of modified dispersion relations. In this peculiar type of dispersion relations, there is an intermediate phase where dispersion relation has a negative slope and results in increasing energy of the modes while their wavelength expands. Still the energy of the modes remain larger than Hubble parameter while they are sub horizon. Even though the modes start from adiabatic vacuum in infinite past, due to this intervening phase, there will be a substantial amount of particle production if the evolved state is mapped to standard Lorentzian modes. Such excited initial states can have interesting phenomenology and it is interesting to know if they are motivated from a more fundamental perspective. We demonstrated that these states can possibly appear within the effective field theory of inflation where the existence of higher dimensional operators naturally leads to the modified dispersion relation. It is interesting to further investigate the bispectrum of such dispersion relations and work out the allowed region of parameters explicitly. The possibility of sixth order and higher dispersion relations were dismissed in the earlier investigations of effective field theory of inflation noting that in the IR they will be strongly decoupled and invalidate the effective field theory description. The argument is based on dimensional energy scaling argument that evaluates the dimension of the goldstone boson scalar field based on dispersion relation. However, in an expanding background, where the higher dimensional terms get redshifted as the universe expands, such dimensional arguments does not seem to be strong. Still, at low energies, the dispersion relation reduces to the Lorentzian one and, a priori, it is not clear that evolution of the mode during the time the physical momentum of the mode is in the new physics region, can lead to effect that makes the effective field theory invalid. In addition, the three point function needs to be compared with the two point function, which as we showed in this article, is by itself large. This analysis is something we plan to return to in future.

Here we also assumed that all the modes that are relevant for the CMB and structure

formation have gone through all three phases of evolution of dispersion relation from the onset of inflation. This would be true if Inflation lasted for the number of e-foldings larger than the minimum number required to solve the problems of standard Big Bang cosmology. In this case, if the largest scale mode that corresponds to our horizon today satisfies this condition, the smaller ones in the CMB have also experienced all three phases of the dispersion relation throughout their evolution. However, the reverse is not necessarily true; if the smaller modes are already in the regime of domination of the k^6 term, the largest mode could have started from k^4 or k^2 regions. Therefore the initial condition which should be set for these modes are not the same as (4.56) and the amplitude of the power spectrum would be different. It would be interesting to investigate the observational consequences of such situations. This is another interesting feature that we plan to get back to in a future study.

Here we only discussed the possibility of generating sextic modified dispersion relations with negative quartic terms from EFT of Inflation for the scalar perturbations. If similar contributions could be generated for tensor perturbations, one can expect similar enhancement for the tensor power spectrum too. Assuming that both tensor and scalar perturbations are affected similarly, that would mean that the tensor-scalar ratio, r, remains intact, but the scale of inflation could be lowered. Then $r \gtrsim 0.01$ would not necessarily correspond to a GUT scale inflation. Investigating whether such dispersion relations is conceivable for tensor perturbations, is another avenue to pursue.

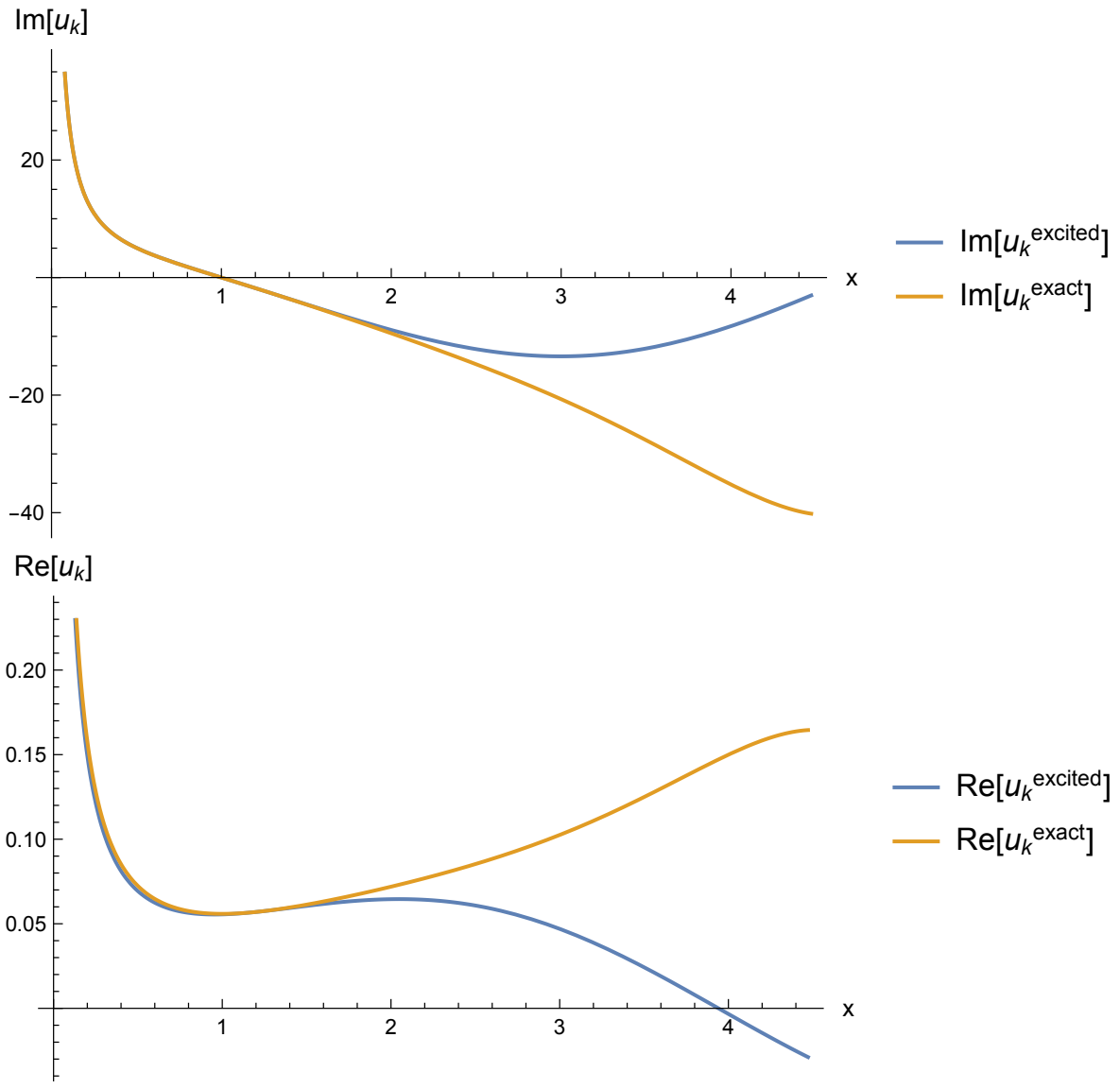

Figure 4.4: Imaginary and real parts of the implicit mode function is compared with the excited state for the choice of a that results in the coalescence of the modes after the collision point.

Chapter 5

Pulsar Data and Constraints on Mass of Particles

5.1 Introduction

The cosmological constant problem is a very well known problem in the field of cosmology. We expect the vacuum energy governed by a ultraviolet cutoff scale Λ to couple to the metric and start accelerated expansion long before any structure can form. However, the observed present time acceleration of expansion requires some sixty orders of magnitude smaller values of vacuum energy [5]. In quantum mechanics, the higher order correlators of stress-energy tensors such as $\left\langle T^{(V)}_{\mu\nu}(x)T^{(V)}_{\mu\nu}(y)\right\rangle$ characterizes the vacuum, while the cosmological constant problem concerns with how the vacuum expectation value of the stress-energy tensor $\left\langle T^{(V)}_{\mu\nu}(x)\right\rangle$ affects the metric. Thus, naturally, the question of how the ultraviolet physics of the vacuum affects space-time geometry in the lower energy scale, so called Cosmological non-Constant problem, arises [5]. Or, simply put, how the two-point correlation function for metric perturbations and the vacuum are related. Thus, in this chapter we will study exactly that, and how the cosmological observations put constraints on high-energy physics.

As a rough analysis and to gain insights of the methodology, we start with two point correlators, which scale as

$$\left\langle T^{(V)}_{ij}(\vec{x})T^{(V)}_{kl}(\vec{y})\right\rangle \sim \delta^3(\vec{x}\vec{y})\Lambda^5, \tag{5.1}$$

where Λ is the cutoff scale. The dimensionless power spectrum Δ^2_Φ of the gravitational potential Φ is given by

$$(\Delta^{(V)}_\Phi)^2 \sim \frac{\Lambda^5}{M_p^4 k}. \tag{5.2}$$

Now requiring $\Delta_\Phi \lesssim 1$ to match with the homogeneity of the universe and approximating $k \sim H_0$, the largest scale, roughly gives

$$\Lambda \lesssim (M_p^4 H_0)^{1/5} \approx 2 \text{ PeV}. \tag{5.3}$$

2 PeV limit on mass is not very meaningful because it's too big. However, we can set strong restrictions using the Cosmic Microwave Background or pulsar data.

5.2 Using Pulsar Data

Pulsars in binary systems have short spin periods, about order of milliseconds, and thus act as a stable precise clocks. Period of these pulsars are incredibly stable, and in some cases can be measured to better than 1 part in 10^{15}. About a decade ago the double-radio pulsar was discovered, providing a unique laboratory for testing Einstein's General Theory of Relativity in the strong field regime. The fact that this double pulsar system PSR J0737-3039A/B comprises two neutron stars, both visible as radio pulsars and also the most relativistic binary pulsar system observed allows very precise testing of general relativity in the strong field regime. The observation and data from this system agrees with the General Theory of Relativity with less than 0.05% uncertainties [42].

In the process of measuring the time of arrival (TOA) for pulses we encounter timing residuals, which is the difference between the observed TOA and predicted values for a model pulsar using TEMPO [42]. The remaining residuals after fitting the residuals with functions representing the model parameters, such as pulsar periods, may be noise. The sources of these timing noises can vary from intrinsic noise of pulsars to perturbations of pulsar motion[42]. In this section, we will view the universe as the semi-classical background and look at metric fluctuation as the source of noise. From there, we will study how double pulsar systems sets a restriction in the mass of particles.

5.2.1 Stress-Energy Correlators

In the section VI of [5], N. Afshordi and E. Nelson calculated spin-0 and spin-2 spectral densities of different fields [5]. For a simple massive scalar field Π with Lagrangian given

by

$$\mathcal{L}_\phi = -\frac{1}{2}[(\partial\phi)^2 + m^2\phi^2], \tag{5.4}$$

we have

$$\begin{aligned}\rho_0^{(\phi)}(-k_4^2) &= \frac{k^4}{144\pi^2}\sqrt{1+4\frac{m^2}{k^2}}\left[\frac{1}{2}-\frac{m^2}{k_4^2}\right]^2\Theta(-k^2-4m^2)\\ \rho_2^{(\phi)}(-k_4^2) &= \frac{k^4}{1920\pi^2}\sqrt{1+4\frac{m^2}{k^2}}\left[\frac{1}{2}-\frac{m^2}{k_4^2}\right]^2\Theta(-k^2-4m^2).\end{aligned} \tag{5.5}$$

Note that in the limit where $k \to 0$ we can ignore Θ function and we get $\rho_2^{(\phi)} = 6\rho_0^{(\phi)}/5$ [4].

For a Dirac field with Lagrangian given by

$$\mathcal{L}_{Dirac} = \bar{\psi}(i\gamma_\mu\partial^\mu - m)\psi, \tag{5.6}$$

we get

$$\rho_0^{(\psi)}(-k^2) = \frac{1}{144\pi^2}m^2(k^2+4m^2)\left(1_{\frac{4m^2}{k^2}}\right)^{1/2}\Theta(-k^2-4m^2), \tag{5.7}$$

where again in the limit $k \to 0$ we have $\rho_2^{(\psi)} = 6\rho_0^{(\psi)}/5$ [4].

For a real massive spin-1 scalar field with Lagrangian

$$\mathcal{L}_A = -\frac{1}{4}F_{\mu\nu}F^{\mu\nu} - \frac{1}{2}m^2A^\mu A_\mu, \tag{5.8}$$

we get

$$\rho_0^{(A)}(-k^2) = \frac{1}{144\pi^2}(3m^4+m^2k^2+\frac{1}{4}k^4)\left(1+\frac{4m^2}{k^2}\right)^{1/2}\Theta(-k^2-4m^2). \tag{5.9}$$

Also note that a complex scalar or a vector field will have a factor of 2 and a Majorana field will be a half of the Dirac field [4].

Now the integration of the step function $\Theta(-k^2-4m^2)$ can be realized in the frequency space. The frequency integral, restricted to $\omega^2 > 4m^2+|\mathbf{k}|^2$ can be deformed in the complex plane [4]:

$$\int_{-\infty}^{\infty} dk_0\Theta(-k^2-4m^2)\times ... = \frac{1}{2}\left(\int_{\mathcal{C}_\infty^+} + \int_{\mathcal{C}_\infty^-} + \int_{\mathcal{C}_{\rm IR}}\right)\times ..., \tag{5.10}$$

where $\mathcal{C}_\infty^\pm$ and $\mathcal{C}_{\rm IR}$ are show in the Figure 5.1. The trick is that when we restrict the integration on real line to $k_0^2 < \Lambda^2$, and take $\Lambda \to \infty$ limit, then $\mathcal{C}_\infty^\pm$ gets divergences in Λ, which vanishes after renormalization, and $\mathcal{C}_{\rm IR}$ converges such that the step function effectively becomes just $-\Theta(k^2)$. Thus the low frequency spectra density is much simplified to

$$\rho_{0,\rm IR}^{(\phi)} = -\frac{1}{72\pi^2}\frac{m^5}{\sqrt{k^2}}\Theta(k^2). \tag{5.11}$$

The relationship between the low frequency spectral density of each field is

$$\rho^{(\psi)} = 4\rho^{(\phi)} = \frac{4}{3}\rho^{(A)}, \tag{5.12}$$

with $\rho_2^{(X)} = \frac{6}{5}\rho_0^{(X)}$.

5.2.2 Pulsar Timing

We will work in the synchronous comoving gauge where the metric is given by

$$ds^2 = -dt^2 + \gamma_{ij}dx^i dx^j. \tag{5.13}$$

The change of energy of a photon moving from $\vec{x}$ to $\vec{x} + \Delta\vec{x}$ is given by

$$\Delta E = -\Gamma^0_{\mu\nu}p^\mu dx^\nu = -\frac{1}{2}\dot{\gamma}_{ij}p^i dx^j. \tag{5.14}$$

Taking time derivative of both sides, we get

$$\frac{\partial \Delta E}{\partial t} = -\frac{1}{2}\ddot{\gamma}_{ij}p^i dx^j = R_{i0j0}p^i dx^j = R_{\mu\nu\alpha\beta}u^\nu u^\beta p^\mu dx^\alpha, \tag{5.15}$$

where $R_{\mu\nu\alpha\beta}$ is a Riemann Tensor and u^μ is the velocity vector. If we sum over all the possible paths from the pulsar to the observer on Earth, we have

$$\frac{dE_{obs}}{dt} = \int_{pulsar}^{Earth} R_{\mu\nu\alpha\beta}u^\nu u^\beta p^\mu dx^\alpha. \tag{5.16}$$

Because the Riemann tensor is first order in curvature, we can consider $p^\mu = E dx^\mu/dt$ and $u^\mu = \delta^\mu_0$ [4]. Then the derivative of log of frequency, ν of the pulsar can be written as

$$\frac{d\ln\nu(t)}{dt} = -\frac{d\ln P(t)}{dt} = u^\nu u^\sigma \frac{dx^\mu}{dt}\frac{dx^\rho}{dt}\int_{t-L}^{t} dt' R_{\mu\nu\rho\sigma}\left[\frac{t-t'}{L}x^i_{pulsar} + \frac{t'-t+L}{L}x^i_{Earth}, t'\right], \tag{5.17}$$

where P is the observed frequency of a pulsar and L is the distance to a pulsar. We can also define the contracted curvature as

$$\bar{R} \equiv u^\nu u^\sigma n^\mu n^\rho R_{\mu\nu\rho\sigma}, \tag{5.18}$$

where $n^\mu = dx^\mu/dt$. The two point function of the contracted curvature is then given by

$$\left\langle\left\langle \bar{R}_k \bar{R}_{k'} \right\rangle\right\rangle = \frac{\pi}{2M_p^4}\frac{1}{k^4}(k\cdot n)^2[k\cdot n + 2(k\cdot u)(n\cdot u)]^2(\rho_0(-k^2) + \frac{8}{3}\rho_2(-k^2)). \tag{5.19}$$

5.2.3 Power Spectrum

The power spectrum of the pulsar period is given by

$$\mathcal{P}(\omega) \equiv \omega^{-2}\int d(\Delta t)\left\langle \frac{d\ln P(t)}{dt}\frac{d\ln P(t')}{dt'}\right\rangle e^{i\omega\Delta t}, \tag{5.20}$$

where $\Delta t = t - t'$ [4]. Furthermore $\mathcal{P}(\omega)$ and the power spectrum of the timing noise Φ_{TN} and the amplitude of the stochastic gravitation waves $h_{c,eq}$ are all related by the equation

$$\mathcal{P}(\omega) = \left(\frac{P\omega}{2\pi}\right)^2 \Phi_{TN} = \frac{h_{c,eq}^2}{6\pi\omega}. \tag{5.21}$$

Now, suppose that we choose a coordinate or an orientation such that the pulsar and Earth is on the z-axis with the observer on Earth as the origin so that $n_\mu = (-1, -\hat{z})$, the equation 5.20 gives, by plugging in eq. 5.17 and 5.18,

$$h_{c,eq}^2 = \frac{12\pi}{\omega}\int \frac{d^3\mathbf{k}}{(2\pi)^3}\left\{\frac{1 - cos[(\omega + k_z)L]}{(\omega + k_z)^2}\right\}\left\langle\left\langle \bar{R}_k \bar{R}_{k'} \right\rangle\right\rangle, \tag{5.22}$$

where $k_z^2 = k^2 - k_\perp^2 + \omega^2$ [4]. Also using the same set up and setting $u_\mu = (-1, \vec{0})$ simplifies the two point correlator for $\bar{R}$

$$\left\langle\left\langle \bar{R}_k \bar{R}_{k'} \right\rangle\right\rangle = \frac{\pi}{2M_p^4}\frac{(k_z^2 - \omega^2)^2}{k^4}\left(\rho_0(-k^2) + \frac{8}{3}\rho_2(-k^2)\right). \tag{5.23}$$

We can also define the effective low frequency spectral density

$$\rho_{eff}^{(X)}(-k^2) = \rho_{0,\mathrm{IR}}^{(X)}(-k^2) + \frac{8}{3}\rho_{2,\mathrm{IR}}^{(X)}(-k^2) = -c_X\frac{7}{120\pi^2}\frac{m^5}{\sqrt{k^2}}\Theta(k^2), \tag{5.24}$$

where

$$\begin{aligned} c_X &= 1 \quad (X = \phi,\ \text{real}) \\ &= 2 \quad (X = \phi,\ \text{complex}) \\ &= 2 \quad (X = \psi,\ \text{Majorana}) \\ &= 4 \quad (X = \psi,\ \text{Dirac}) \\ &= 3 \quad (X = A_\mu,\ \text{real}) \\ &= 6 \quad (X = A_\mu,\ \text{complex}). \end{aligned} \tag{5.25}$$

We can finally evaluate the equation 5.22 to get

$$\begin{aligned} (h^2_{c,eq})^{(X)} &\approx -c_X \frac{7}{480\pi^3} \frac{m^5}{M_p^4 \omega} \left[\sqrt{4\pi\omega L} + \ln\left(K_{max} L\right)\right] \\ &\approx -4 \times 10^{-30} c_X \left(\frac{m}{600\text{GeV}}\right)^5 \sqrt{\frac{2\pi L(\text{kpc})}{\omega(\text{yr}^{-1})}}, \end{aligned} \tag{5.26}$$

where k_{max} is the cut off for k_z such that $|k_z| < k_{\text{max}}$. Notice that in the second line the $\mathcal{O}(1)$ contribution from the term $\ln(k_{\text{max}} L)$ has been dropped.

Since we have equations for $h^2_{c,eq}$ and the values of Φ_{TN}, P, and ω [50] [48], we can plug the values to get the values for m. The least 2σ upper bound was $m < 420$GeV for complex vectors and the highest bound was given by the real scalar at $m < 600$GeV. Table 5.1 shows the 2σ upper bounds for different type of fields and Figure 5.2 shows the upper bound of real scalars given by different pulsar data.

Beyond-SM Mass Bounds

Particle Species	2σ *upper bound*
Real Scalar	$m < 600$ GeV
Complex Scalar	$m < 525$ GeV
Majorana	$m < 525$ GeV
Dirac	$m < 450$ GeV
Real Vector	$m < 480$ GeV
Complex Vector	$m < 420$ GeV

Table 5.1: Mass bounds on Beyond Standard Model particles of different species, from PSR J1909-3744.

5.3 Summary and Future Works

Here we started from how the fluctuation of the cosmological constant, albeit the constant itself can be small, can become large and modify how our universe can look in the current era. Instead of attempting to resolve the issue, we looked at observational data and how that sets constraints on to the models and theories at high energies. Afshordi and Nelson, showed that the CMB data sets restriction on how big the vacuum fluctuation can be in the early universe, and thus computed the upper bound on mass of particles to be less than 35 TeV [5].

In this chapter, we took the similar approach. We briefly showed how Afshordi and Nelson used the CMB data to mathematically compute the upper bound of mass. Using a similar approach we set upper bounds to mass using 11 different pulsar data. We used the relationship between the timing noise of pulsars, the metric fluctuations, and the vacuum stress-energy correlators to analyze the upper bound for mass of particles. We have computed that the lowest 2σ upper bound is 420 GeV for complex vector fields, and the highest elementary particle found is a top quark at 173 GeV. Fortunately since there are more telescopes and particle colliders being built in the future, we should be able to test our result more rigorously and learn more about the physics beyond the standard model.

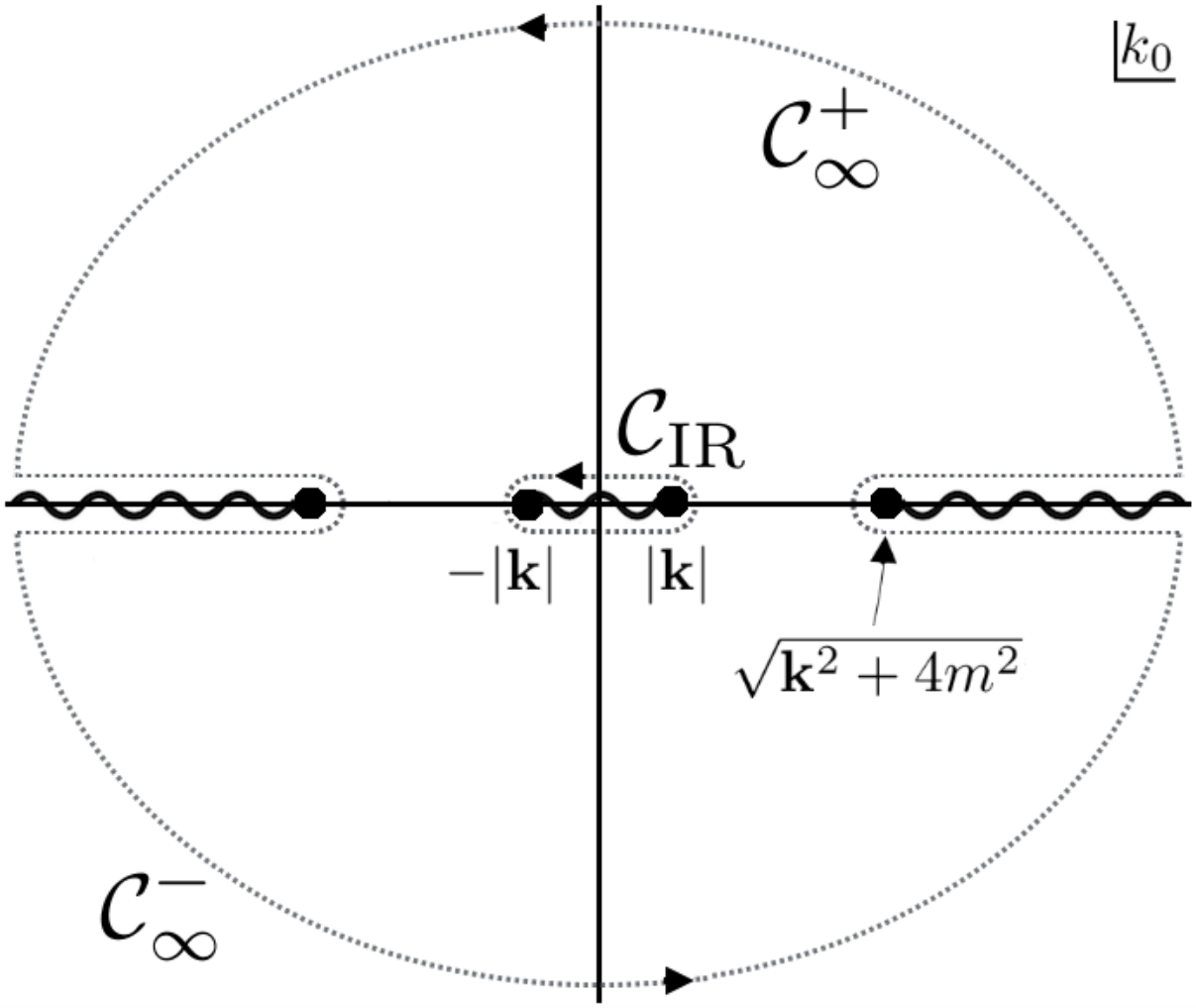

Figure 5.1: The frequency integral in complex plane. The contours at infinity $\mathcal{C}_\infty^\pm$ and the low frequency contours $\mathcal{C}_{IR}$ is shown.

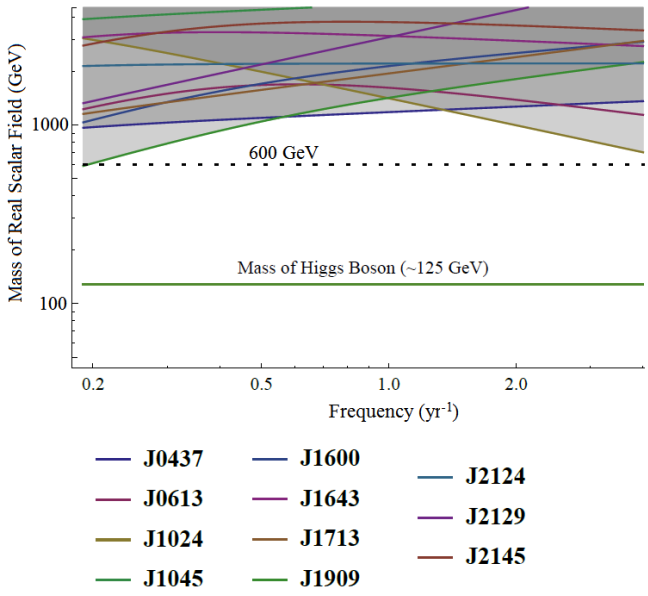

Figure 5.2: This graph shows the mass bounds given by the timing noise of different pulsars for the real scalar field. The 11 different pulsars were chosen [48]. The least mass bound was given by PSR J1901-3744 at $f \approx 0.2$ yr^{-1}. Mass bounds on higher-spin particles are slightly stronger (see Table 5.1).

Chapter 6

Conclusion

We started by introducing the key concepts and theories and also the challenges in the current models in cosmology in the chapter 2. In chapter 3 and 4, the attempt to resolve those questions were made by using different models and approaches. Thus, the non-canonical scalar cuscuton was introduced, and the effective field theory approach of inflation was also mentioned. Although in chapter 3, we did not suggest a theory or model which helps answering puzzles that the inflationary scenarios have, the rigorous calculation of second order action with cuscuton can help probing non inflationary models, such as bounce scenarios. In chapter 4, we noticed that from modified dispersion relations could lead to different initial states. Furthermore, we showed that the effective field theory of inflation could give us the modification on dispersion relations that we were looking for. In chapter 5, how a problem, yet unanswered, still sets a limit to our models by using the observational data. This thesis, in essence, aimed to provide basic background of cosmology, the challenges it's facing and the community's effort to finding possible ways to answer them. And this concludes the work. Thank you for reading.

References

[1] P. A. R. Ade et al. Planck 2015 results. XX. Constraints on inflation. *Astron. Astrophys.*, 594:A20, 2016.

[2] Niayesh Afshordi, Daniel J. H. Chung, Michael Doran, and Ghazal Geshnizjani. Cuscuton Cosmology: Dark Energy meets Modified Gravity. *Phys. Rev.*, D75:123509, 2007.

[3] Niayesh Afshordi, Daniel J. H. Chung, and Ghazal Geshnizjani. Cuscuton: A Causal Field Theory with an Infinite Speed of Sound. *Phys. Rev.*, D75:083513, 2007.

[4] Niayesh Afshordi, Hyungjin Kim, and Elliot Nelson. Pulsar Timing Constraints on Physics Beyond the Standard Model. 2017.

[5] Niayesh Afshordi and Elliot Nelson. Cosmological Non-Constant Problem: Cosmological bounds on TeV-scale physics and beyond. In *Meeting of the APS Division of Particles and Fields (DPF 2015) Ann Arbor, Michigan, USA, August 4-8, 2015*, 2015.

[6] Gian Luigi Alberghi, Roberto Casadio, and Alessandro Tronconi. Planck scale inflationary spectra from quantum gravity. *Phys. Rev.*, D74:103501, 2006.

[7] R. Arnowitt, S. Deser, and C. W. Misner. Dynamical structure and definition of energy in general relativity. *Phys. Rev.*, 116:1322–1330, Dec 1959.

[8] A. Ashoorioon, J. L. Hovdebo, and Robert B. Mann. Running of the spectral index and violation of the consistency relation between tensor and scalar spectra from trans-Planckian physics. *Nucl. Phys.*, B727:63–76, 2005.

[9] A. Ashoorioon, Achim Kempf, and Robert B. Mann. Minimum length cutoff in inflation and uniqueness of the action. *Phys. Rev.*, D71:023503, 2005.

[10] A. Ashoorioon and Robert B. Mann. On the tensor/scalar ratio in inflation with UV cut off. *Nucl. Phys.*, B716:261–279, 2005.

[11] Amjad Ashoorioon, Roberto Casadio, Ghazal Geshnizjani, and Hyung J. Kim. Getting Super-Excited with Modified Dispersion Relations. 2017.

[12] Amjad Ashoorioon, Roberto Casadio, and Tomi Koivisto. Anisotropic non-Gaussianity from Rotational Symmetry Breaking Excited Initial States. *JCAP*, 1612(12):002, 2016.

[13] Amjad Ashoorioon, Diego Chialva, and Ulf Danielsson. Effects of Nonlinear Dispersion Relations on Non-Gaussianities. *JCAP*, 1106:034, 2011.

[14] Amjad Ashoorioon, Konstantinos Dimopoulos, M. M. Sheikh-Jabbari, and Gary Shiu. Non-BunchDavis initial state reconciles chaotic models with BICEP and Planck. *Phys. Lett.*, B737:98–102, 2014.

[15] Amjad Ashoorioon, Konstantinos Dimopoulos, M. M. Sheikh-Jabbari, and Gary Shiu. Reconciliation of High Energy Scale Models of Inflation with Planck. *JCAP*, 1402:025, 2014.

[16] Amjad Ashoorioon and Tomi Koivisto. Hemispherical Anomaly from Asymmetric Initial States. *Phys. Rev.*, D94(4):043009, 2016.

[17] Amjad Ashoorioon and Gary Shiu. A Note on Calm Excited States of Inflation. *JCAP*, 1103:025, 2011.

[18] John M. Lee (auth.). *Introduction to Smooth Manifolds*. Graduate Texts in Mathematics 218. Springer New York, version 3.0 draft edition, 2003.

[19] Daniel Baumann. Inflation. In *Physics of the large and the small, TASI 09, proceedings of the Theoretical Advanced Study Institute in Elementary Particle Physics, Boulder, Colorado, USA, 1-26 June 2009*, pages 523–686, 2011.

[20] D. Bessada, W. H. Kinney, D. Stojkovic, and J. Wang. Tachyacoustic cosmology: An alternative to inflation. *Phys. Rev. D*, 81(4):043510, feb 2010.

[21] Supranta S. Boruah, Hyung J. Kim, and Ghazal Geshnizjani. Theory of Cosmological Perturbations with Cuscuton. *JCAP*, 1707(07):022, 2017.

[22] Robert H. Brandenberger. Lectures on the theory of cosmological perturbations. *Lect. Notes Phys.*, 646:127–167, 2004. [,127(2003)].

[23] Sean Carroll. *Spacetime and geometry: an introduction to General Relativity*. Benjamin Cummings, 2004.

[24] Aidan Chatwin-Davies, Achim Kempf, and Robert T. W. Martin. Impact of Natural Planck Scale Cutoffs that are Fully Covariant on Inflation. 2016.

[25] Clifford Cheung, Paolo Creminelli, A. Liam Fitzpatrick, Jared Kaplan, and Leonardo Senatore. The Effective Field Theory of Inflation. *JHEP*, 03:014, 2008.

[26] Nora Elisa Chisari, Cora Dvorkin, Fabian Schmidt, and David Spergel. Multitracing Anisotropic Non-Gaussianity with Galaxy Shapes. *Phys. Rev.*, D94(12):123507, 2016.

[27] Steven Corley and Ted Jacobson. Hawking spectrum and high frequency dispersion. *Phys. Rev.*, D54:1568–1586, 1996.

[28] G. D'Amico, C. de Rham, S. Dubovsky, G. Gabadadze, D. Pirtskhalava, and A. J. Tolley. Massive Cosmologies. *Phys. Rev.*, D84:124046, 2011.

[29] Ulf H. Danielsson. A Note on inflation and transPlanckian physics. *Phys. Rev.*, D66:023511, 2002.

[30] Richard Easther, Brian R. Greene, William H. Kinney, and Gary Shiu. Inflation as a probe of short distance physics. *Phys. Rev.*, D64:103502, 2001.

[31] Richard Easther, Brian R. Greene, William H. Kinney, and Gary Shiu. A Generic estimate of transPlanckian modifications to the primordial power spectrum in inflation. *Phys. Rev.*, D66:023518, 2002.

[32] Richard Easther, Brian R. Greene, William H. Kinney, and Gary Shiu. Imprints of short distance physics on inflationary cosmology. *Phys. Rev.*, D67:063508, 2003.

[33] Brian R. Greene, Koenraad Schalm, Gary Shiu, and Jan Pieter van der Schaar. Decoupling in an expanding universe: Backreaction barely constrains short distance effects in the CMB. *JCAP*, 0502:001, 2005.

[34] Alan H. Guth. Inflationary universe: A possible solution to the horizon and flatness problems. *Phys. Rev. D*, 23:347–356, Jan 1981.

[35] Petr Horava. Quantum Gravity at a Lifshitz Point. *Phys. Rev.*, D79:084008, 2009.

[36] S. E. Joras and G. Marozzi. Trans-Planckian Physics from a Non-Linear Dispersion Relation. *Phys. Rev.*, D79:023514, 2009.

[37] Yonatan Kahn, Daniel A. Roberts, and Jesse Thaler. The goldstone and goldstino of supersymmetric inflation. *JHEP*, 10:001, 2015.

[38] Nemanja Kaloper, Matthew Kleban, Albion E. Lawrence, and Stephen Shenker. Signatures of short distance physics in the cosmic microwave background. *Phys. Rev.*, D66:123510, 2002.

[39] Achim Kempf. Mode generating mechanism in inflation with cutoff. *Phys. Rev.*, D63:083514, 2001.

[40] Achim Kempf and Jens C. Niemeyer. Perturbation spectrum in inflation with cutoff. *Phys. Rev.*, D64:103501, 2001.

[41] D. Langlois. Lectures on inflation and cosmological perturbations. *Lect. Notes Phys.*, 800:1–57, 2010.

[42] R. N. Manchester. Pulsars and Gravity. *Int. J. Mod. Phys.*, D24(06):1530018, 2015.

[43] Jerome Martin and Robert Brandenberger. On the dependence of the spectra of fluctuations in inflationary cosmology on transPlanckian physics. *Phys. Rev.*, D68:063513, 2003.

[44] Jerome Martin and Robert H. Brandenberger. The TransPlanckian problem of inflationary cosmology. *Phys. Rev.*, D63:123501, 2001.

[45] Jerome Martin and Robert H. Brandenberger. The Corley-Jacobson dispersion relation and transPlanckian inflation. *Phys. Rev.*, D65:103514, 2002.

[46] V. F. Mukhanov, H. A. Feldman, and R. H. Brandenberger. Theory of cosmological perturbations. *Phys. Rev.*, 215:203–333, Jun 1992.

[47] Arno A. Penzias and Robert Woodrow Wilson. A Measurement of excess antenna temperature at 4080-Mc/s. *Astrophys. J.*, 142:419–421, 1965.

[48] D. J. Reardon et al. Timing analysis for 20 millisecond pulsars in the Parkes Pulsar Timing Array. *Mon. Not. Roy. Astron. Soc.*, 455(2):1751–1769, 2016.

[49] Leonardo Senatore. Lectures on Inflation. In *Proceedings, Theoretical Advanced Study Institute in Elementary Particle Physics: New Frontiers in Fields and Strings (TASI 2015): Boulder, CO, USA, June 1-26, 2015*, pages 447–543, 2017.

[50] R. M. Shannon et al. Gravitational waves from binary supermassive black holes missing in pulsar observations. *Science*, 349(6255):1522–1525, 2015.

[51] Gary Shiu and Ira Wasserman. On the signature of short distance scale in the cosmic microwave background. *Phys. Lett.*, B536:1–8, 2002.

[52] Ashish Shukla, Sandip P. Trivedi, and V. Vishal. Symmetry constraints in inflation, α-vacua, and the three point function. *JHEP*, 12:102, 2016.

[53] Witold Skiba. Effective Field Theory and Precision Electroweak Measurements. In *Physics of the large and the small, TASI 09, proceedings of the Theoretical Advanced Study Institute in Elementary Particle Physics, Boulder, Colorado, USA, 1-26 June 2009*, pages 5–70, 2011.

[54] Takahiro Tanaka. A Comment on transPlanckian physics in inflationary universe. 2000.

[55] Tao Zhu, Anzhong Wang, Klaus Kirsten, Gerald Cleaver, and Qin Sheng. High-order Primordial Perturbations with Quantum Gravitational Effects. *Phys. Rev.*, D93(12):123525, 2016.